UNIVERSITÉ DU QUÉBEC À MONTRÉAL

CONTROLLED CVD GROWTH OF TWO-DIMENSIONAL MOS_2 FILMS

DISSERTATION
PRESENTED
AS PARTIAL REQUIREMENT
TO THE MASTERS IN CHEMISTRY

BY

DALAL SHARATA

AUGUST 2018

UNIVERSITÉ DU QUÉBEC À MONTRÉAL

LA CROISSANCE CONTRÔLÉE DU MATÉRIAU MoS_2 PAR CVD

MÉMOIRE
PRÉSENTÉ
COMME EXIGENCE PARTIELLE
DE LA MAÎTRISE EN CHIMIE

PAR

DALAL SHARATA

AOÛT 2018

ACKNOWLEDGMENTS

First of all, I would like to express gratitude to my supervisor Prof Mohamed Siaj for supporting me during my time and, also giving me the opportunity to complete my master's degree in his research group.

I would like to thank Dr sujittra poorahong for helping me throughout my master's and spending a lot of time training me for all the characterization techniques.I would like to extend special thanks to Madam soina Lachance,who helped me through all my studies.
I would like to thank all my friends and all Siaj group for sharing a device Mohamed, Ahamed Abdallah, Manel, Siham, Ons, Wassila, Farzaneh, Thai and Somia.

I would like to thank my family and sibling for pushing me to continue my studies, there were always giving me supporting and encouraging me with their nice wishes. I must express my gratitude to my husband Safwan, for helping me and stand beside me through my studying, and also my lovely children.

Finally, I would like to acknowledge the high ministries of Libyan government of the scholarship was giving to me this opportunity to complete my master's degree in Canada.

DEDICATION

I would like to dedicate this work to my lovely husband Safwan Khalil. There is no doubt in my mind that without his advice and support I could not have to finish this work. A special feeling of gratitude to my loving parents, Mohammed Sharata and Mabroka Alharary whose words of encouragement and push for tenacity rings in my ears, all my brothers and sisters have never left my side and very special. I dedicate this work and give special thanks to my best supervisor Mohamed Siaj and all Siaj groups and all my best friend Dalal Al-Hattab, Fatme Eljetlawi, and my wonderful children Larin, Areen, and Rana for being there for me throughout the entire Master degree.

TABLE OF CONTENTS

LIST OF FIGURES

Figure Page

LIST OF TABLES

Table Page

LIST OF ABBREVIATIONS, SYMBOLS AND ACRONYMS

CVD	Chemical Vapor Deposition
2D	Two - dimensional
TMDS	Transitional Metal Dichalcogenides
MoS_2	Molybdenum di sulfide
MoO3	Molybdenum trioxide
Mo	Molybdenum
S	Sulfur
Ar	Aryl ring
SiO_2/Si	scion dioxide
SEM	Scanning Electron Microscopy
AFM	Atomic Force Microscopy
XPS	X-ray Photoemission Spectroscopy
PL	Photoluminescence
FET	field-effect transistors
IPA	isopropanol
H2So4	Sulfuric acid
H2O2	Hydrogen peroxide
Au	Gold

LIST OF UNITS

C^0	Temperature
Min	Minutes
H	Hour
Nm	Nanometer
G	Gram
Sccm	Standard Cubic Centimeters per
T	Time
V	Voltage
μ	Micro
eV	Electronvolt

RÉSUMÉ

Les matériaux 2D tels que les monocouches de dichalcogénures de métaux de transition (TMDs) ont attiré beaucoup d'attention en raison de leurs propriétés électroniques uniques et de leurs utilisations potentielles dans diverses applications en optique et en optoélectronique. Ces dichalcogénures représentent une alternative aux autres types de matériaux 2D tels que le graphène.

Les monocouches de dichalcogénures de métaux de transition adoptent une structure simple de formulation MX_2 (M = Mo, W, X = S, Se). Ces matériaux MX_2 sont tous des composés lamellaires et composés de feuillets bidimensionnels similaires à celle du graphite. Chaque feuillet est composé des cations métalliques M insérés entre deux plans d'anions X. Les liaisons M-X sont de nature covalente, tandis que les liaisons entre feuillets sont de types Van der Waals.

Dans le présent projet, le dépôt chimique en phase vapeur (CVD) a été utilisé pour synthétiser le disulfure de molybdène (MoS_2) à différentes températures. La qualité du MoS_2 obtenue à diverses conditions de croissance a été systématiquement étudiée. Dans ce sens, des méthodes de caractérisation de surfaces telles que la spectroscopie et la cartographie Raman, la microscopie électronique à balayage (MEB), l'imagerie optique, la microscopie à force atomique (AFM) et la spectrométrie photo-électronique de rayon X ont été utilisées.

Ce travail de recherche présente une méthode simple et efficace pour réaliser la croissance des matériaux 2D tels que le MoS_2 sur un substrat solide (SiO_2/Si). Le MoS_2 possède une largeur de bande appréciable en tant que couches actives pour des applications reliées à l'électronique logique et l'optoélectronique. Ce type de matériau peut également être une composante active pour diverses applications liées à la production de l'énergie propre comme l'hydrogène.

Mots-clés: Croissance de MoS_2, Déposition Chimique en Phase Vapeur, Métal de Transition Dichalcogénures, Transistor à Effet de Champs

ABSTRACT

Two-dimensional (2D) materials such as Transitional Metal Dichalcogenides (TMDS) have attracted much attention due to their unique properties and great potential in various applications for next generation in electronics and optoelectronics devices relying on ultimate atomic thicknesses. Transition metal dichalcogenides represent an alternative group of 2D layered materials that differ from the semimetallic character of graphene. Few-layered TMDs, in a common form of MX_2 (M = Mo, W; X = S, Se), exhibit numerous fascinating properties associated with their reduced thickness.

In the present project, we are using the Chemical Vapor Deposition (CVD) technique to syntheses MoS_2 layers at different growth temperatures. The quality of the synthesized MoS_2 was systematically investigated with various growth conditions. A detailed analysis of the CVD grown MoS_2 layers was performed, including Raman spectroscopy, Raman mapping, scanning electron microscopy (SEM), optical imaging, atomic force microscopy (AFM), and X-ray photoemission spectroscopy (XPS).

In this study, we are demonstrating a simple and effective method to synthesize MoS_2 on the solid substrate (SiO_2/Si). The MoS_2 material is a sizable band gap which is suitable as active layers in logic electronics and optoelectronics and as constituents in a variety of energy-related applications like hydrogen evolution reaction (HER).

Key word : Growth of MoS_2, Chemical Vapor Deposition, Transitional Metal Dichalcogenides, Field-Effect Transistors.

MISE EN CONTEXTE

Ce projet est consacré à la croissance et l'évaluation du potentiel des monocouches du disulfure de molybdène (MoS_2) en tant qu'un semi-matériau de type N. Ce semi-conducteur d'épaisseur nanométrique est stable chimiquement, robuste mécaniquement, et possède une bande directe de 1.9 eV.

La première partie de ce projet été consacré au dépôt chimique en phase vapeur (CVD) des monocouches du molybdène disulfure. Plusieurs paramètres tels que la température de four, le temps de croissance, le débit de gaz porteur et le nombre de fours utilisés ont été étudiés afin de trouver des conditions optimales de croissance de ce matériau.

L'utilisation d'une nouvelle stratégie à deux fours pour la croissance de MoS_2 a permis l'obtention du MoS_2 de grande qualité par CVD. L'optimisation des paramètres de synthèse a permis une productibilité de la croissance de MoS_2 au laboratoire. En ajustant les conditions de synthèse, nous avons pu obtenir deux types de morphologies du matériau MoS_2. Un type sous forme de multicouches ayant une surface de l'ordre du cm^2 de MoS_2 et un type avec des domaines individuels sous forme de monocouche de forme triangulaire .

Les méthodes de caractérisation de surfaces telle que la spectroscopie et la cartographie Raman, la microscopie électronique à balayage (MEB), l'imagerie optique, la microscopie à force atomique (AFM) et la Spectrométrie photo-électronique de rayon X ont été utilisés pour effectuer une étude approfondie du MoS_2 synthétisé par CVD.

La deuxième partie de ce projet a été consacré à l'intégration de MoS_2 dans des transistors. Pour la fabrication des dispositifs , un dépôt des électrodes sur la surface de

MoS_2 a été réalisé. L'évaporation du métal (Au/Cr) est principalement utilisée comme une méthode de dépôt des électrodes dans ce travail. En utilisant un simple masque perforé, des électrodes en Au/Cr ont été déposés par évaporation thermique avec succès sur la surface de MoS_2 préalablement préparée.

Les mesures de différentes courbes électriques pour la mobilité des porteurs de charges (Caractéristiques de sorties (Id-Vd) et de transfert (Id-Vg)) ont été réalisées. Nous avons trouvé que les mobilités électroniques sont de l'ordre de 0.11-8.4 $cm^2/V.S$.

Ce travail de recherche expose une méthode simple et efficace pour la synthèse de MoS_2 sur un substrat solide (SiO_2/Si). Le MoS_2 possède une largeur de bande appréciable en tant que couches actives pour des applications reliées à l'électronique logique et l'optoélectronique. Ce type de matériau peut également être une composante active pour diverses applications liées à l'énergie et aux capteurs de gaz.

CHAPITRE I

GENERALITÉS

1.1 Transition-Metal Dichalcogenides (TMDs)

Two-dimensional (2D) materials such as Transitional Metal Dichalcogenides (TMDs) have attracted much attention due to their unique properties and great potential in various applications. Since the first report concerning the discovery of the graphene material in 2004 (K. S. Novoselov et al., 2004), two-dimensional (2D) materials have become one of the most active research fields leading to many applications like photocatalysts (Z. Zeng et al., 2011), photo sensors (Lopez-Sanchez, Lembke, Kayci, Radenovic, & Kis, 2013) and field-effect transistors (FET),(Radisavljevic, Radenovic, Brivio, Giacometti, & Kis, 2011). Indeed, it found that the FET transistor based single TMDs monolayer semiconductor behavior with high on/off ratios and mobility at room temperature (britton W.H Baugher, Hugh O.H (5)), (Baugher, Churchill, Yang, & Jarillo-Herrero, 2013).

Few-layered TMDs, in a common form of MX_2 (M = Mo, W; X = S, Se), (Ma, Kou, Li, Dai, & Heine, 2016) exhibit numerous fascinating properties associated with their reduced thickness. MoS_2 can be grown successfully by chemical vapor deposition (CVD) method on top of SiO_2/Si substrate by using molybdenum trioxide (MoO_3) and Sulfur (S) powders as precursors. In this work, we focused on MoS_2 synthesis at the different growth temperature. CVD is known to be the most efficient method for large-area MoS_2 films growth. The advantages of using CVD method are, the low cost, easy

to use and highly reliable technique. Different techniques are used in this study to characterize the resulting MoS_2 films, like atomic force microscope (AFM), X_ray photoelectron spectroscopy (XPS), scanning electron microscope (SEM), Raman spectroscopy and Raman mapping. MoS_2 has been widely used in the preparation of the nano electrodes in recent years. In this study, we focused on the MoS_2 single layer CVD growth.

Transition metal dichalcogenides (TMDs), such as MoS_2, WS_2, $MoSe_2$, and WSe_2 (Wang, Kalantar-Zadeh, Kis, Coleman, & Strano, 2012) are considered to be the family of nanomaterials which their chemical and physical properties are used for many applications such as optoelectronic and electronic applications (Ma et al., 2016), (Radisavljevic et al., 2011), (Radisavljevic et al., 2011). TMDs are flexible and stretchable 2D materials. In addition, these 2D materials are considered as soft semiconductors with a direct band gap in contrast to their well-known bulk crystals that are rigid and hard with indirect band gap (Lee et al., 2012).

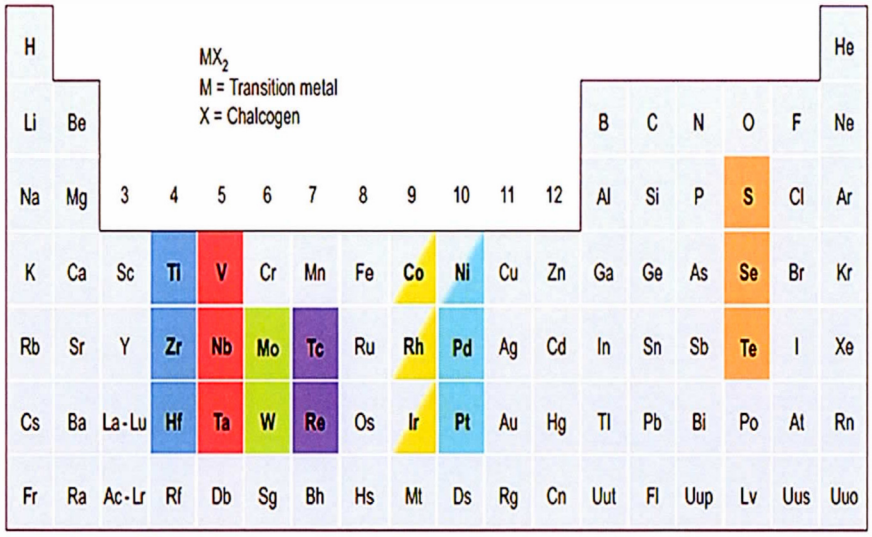

Figure 1.1 Table shown the TMDs' family and the chalcogen elements

1.2 Structure of Monolayer TMDs

The structure of monolayer TMDs is different than graphene. TMDs are not monolayered but in reality consist of three layers. The transition metal atoms are sandwiched between two layers of chalcogen atoms on top and chalcogenides beneath (S-Mo-S) whereas the middle layer is Mo (Tedstone et al., 2015), (W.-b. Xu et al., 2014). This specific structure makes them more stable and flexible with improved semiconducting, metallic and superconducting properties (Radisavljevic et al., 2011), see the structure of TMDs with a side view, top view and possible triangular prismatic structure (Figure 1.2). The top view structure is similar to graphene and exhibiting a hexagonal shape, in which a triangular prismatic it one atom of transition–metal surrounded together with six chalcogen atoms (Ataca, Sahin, & Ciraci, 2012).

Crystal structures of TMDs

A MX_2: (M: Mo, W X: S, Se, Ti)

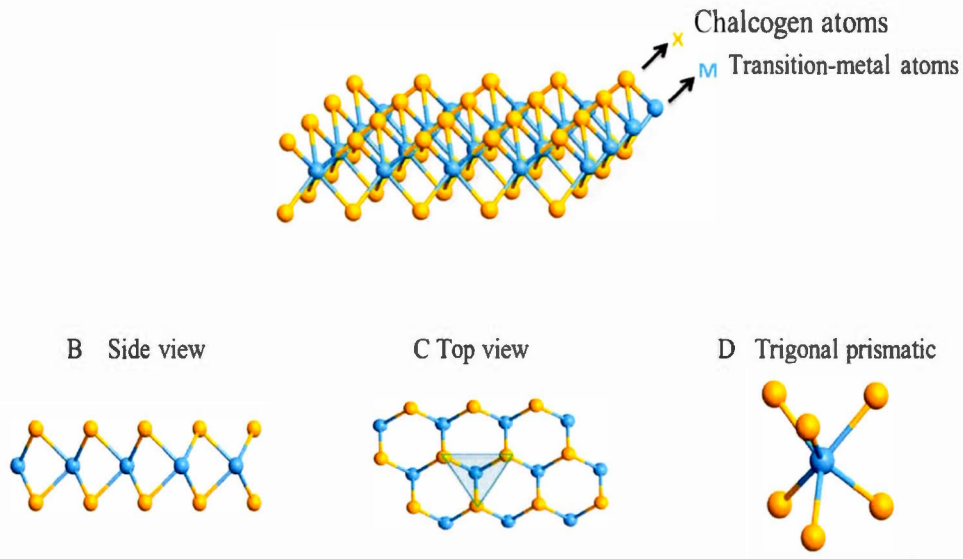

Figure 1.2 The structure of monolayer TMDs side and top views. Chalcogen atoms are shown in yellow and transition metal atoms are shown in blue color

There are three crystal structures of TMDs monolayer's : 2H, 1T and 3R (Dungey, Curtis, & Penner-Hahn, 1998) (see figure 1.3). 2H phase is the most stable phase, 1T phase refers to bulk crystals and 3R phase is for octahedral prismatic phase (Y. Li, Duerloo, Wauson, & Reed, 2016).

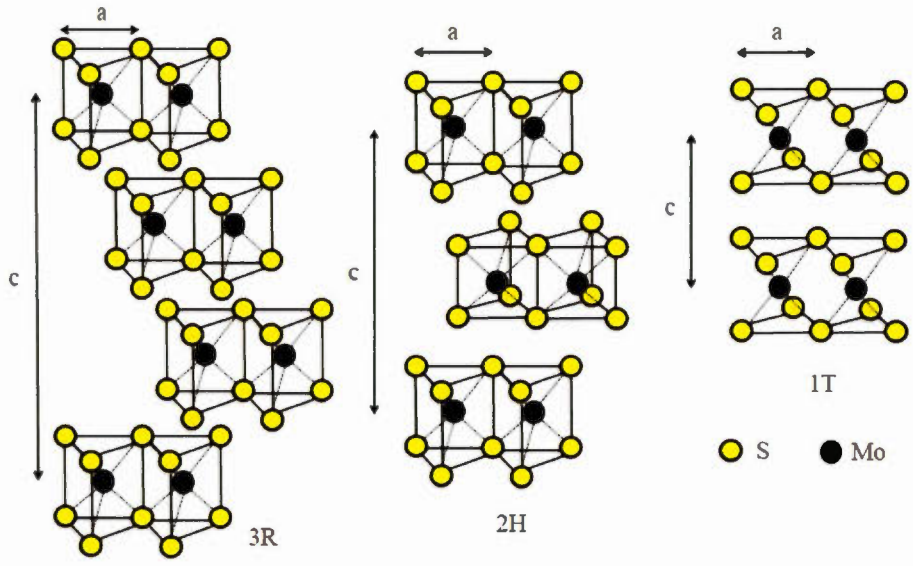

Figure 1.3 Shows a typical three structures of TMDs resulting from different phases: 3R, 2H, and 1T. (a and c are the in-plane and out-of-plane), (Sheu, 2015)

1.3 Classification of Van der Waals 2D material heterostructures

The Van der Waals heterostructures and the classification of 2D materials are shown in Figure 1.4. For instance, graphene has zero band gap and Boron nitride hBN as an excellent insulator with higher band gaps around 5.5 eV (Song et al., 2010). However, MoS_2 is well known to be a semiconductor with a depending change of band gap from indirect band gaps about 1.2 eV for the bulk MoS_2 and a direct band gap around 1.9 eV for monolayer (Kuc, Zibouche, & Heine, 2011). Figure 1.5 shows the difference between direct and an indirect band gap of material.

Material	Structure	Bandgap
Graphene	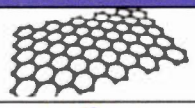	0
h-BN	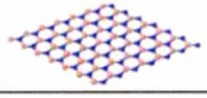	~7.2 eV (indirect)
TMD (MX_2) M: W, Mo, Hf, Zr, Ti, Cr, Ta X: S, Se, Te	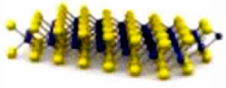	0.6 – 2.3 eV, and depending on layer #
Black Phosphorus (BP)		~2 eV (Monolayer) ~0.3eV (few layer)

Figure 1.4 Graphene and beyond: Two-Dimensional Materials can cover a broad range of wavelengths.

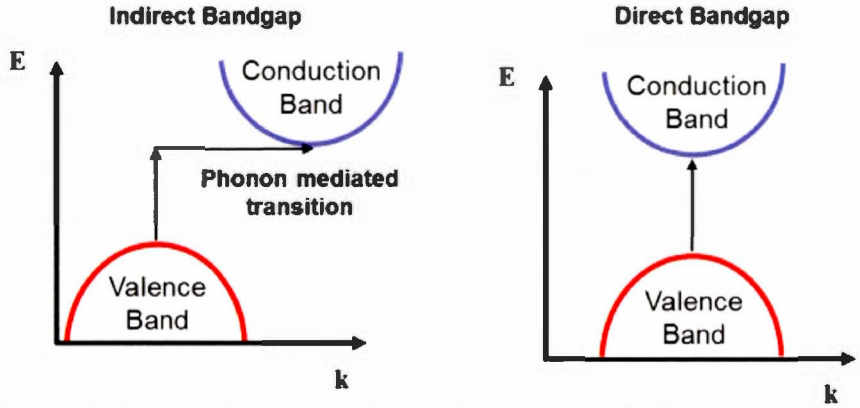

Figure 1.5 Shows the comparison of direct and an indirect band gap of 2D materials. E is the energy and k is the wavenumber (Jacobs-Gedrim, 2015)

1.4 The applications of TMDs 2D materials

MoS_2 is one of the most important inorganic compounds of TMDs 2D materials family. MoS_2 exhibits interesting optical, chemical and physical properties as well as the depending change of band gap from indirect to direct band gap with high mobility of high on/off ratio (~108) (Radisavljevic et al., 2011). TMDs they have many advantages because of their sizable band gap, which makes them good candidates for the future semiconductor devices (Taheri, 2015). Figure 1.6 shows some applications that could be done by using these new generation 2D materials. In addition, MoS_2 has many notations as an electrode material for water splitting (Li et al., 2011), (Kibsgaard, Chen, Reinecke, & Jaramillo, 2012). Therefore, there are many promising applications of thin TMDs such as field effect transistors of single layer MoS_2 showing mobility on the order 1 $cm^2 V^{-1} s^{-1}$ at room temperature (K.-K. Liu et al., 2012), (Radisavljevic et al., 2011), (Yin et al., 2011).

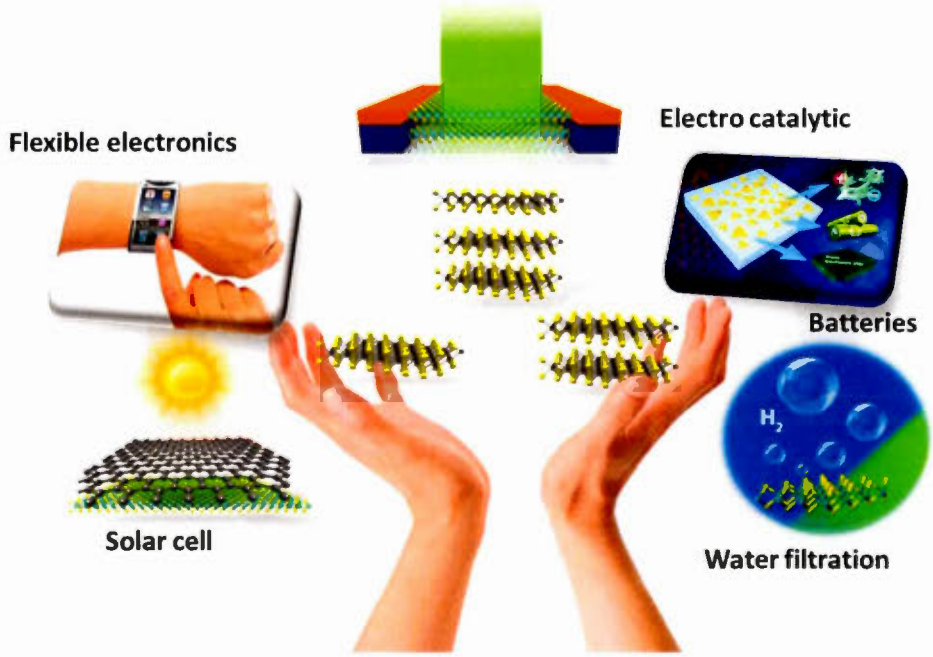

Figure 1.6 The applications of 2D materials based TMDs (Lv et al., 2014)

1.5 The chemical and the physical properties of MoS_2

MoS_2 has the following structure S –Mo –S, two atoms of S and one atom of Mo as a sandwich structure with weak Van der Waals forces (K. S. Novoselov et al., 2004). However, the bonding between Mo and S is stronger. MoS_2 is one of the TMDs more popular 2D materials and the most investigated semiconductor in TMDs field in which its properties change by changing from indirect to direct band gap. Therefore MoS_2 is not only a good candidate for its chemical properties, flexibility and stability but also excellent candidate for its optical and electrical appatications (Chhowalla et al., 2013),

(Huang, Zeng, & Zhang, 2013) and (Shi, Li, & Li, 2015). For more information regarding the chemical and physical proprieties see tables 1.1 and 1.2.

Table 1.1 The chemical properties of MoS_2 nanoparticles

Properties	Molybdenum MoS_2	Sulfur S
Electronic configuration	Mo (Ramakrishna Matte et al.) $4d^5\ 5s^1$	S (Lin et al.) $3s^2\ 3p^4$
Group	Mo group 6	S group 16
Chemical Composition	59.94	40.05

Table 1.2 The physical properties of MoS_2 nanoparticles

Properties	Metric	Imperial
Density	5.06 g/cm^3	0.18216/in^3
Molar mass	160.07 g/mol	-
Melting point	1185 °C	2165 °F

(NANO, 12 july 2013)

1.6. MoS_2 synthesis by different methods

1.6.1 Mechanical Exfoliation

As the case of graphene material (K. Novoselov et al., 2005), mechanical exfoliation of bulk material was used to produce monolayers and multilayered TMDs flakes. In this way, to exfoliate the bulk material, scotch tape has been used. Normally, it is very easy to peel off layers of the source material because of the weak interlayer coupling between layers. As part of peel off the process, the substrate is attached to layers of 2D material.This is quite simple as well as non-costive, as the only equipment that is needed is a Scotch Tape (see Figure 1.7) (Lopez-Sanchez et al., 2013).

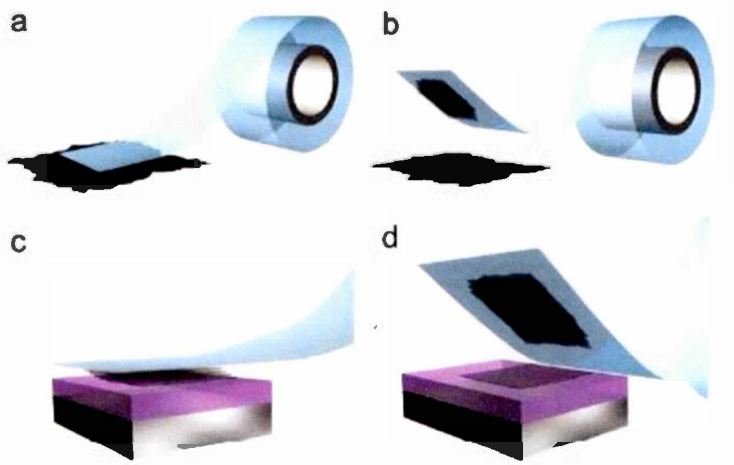

Figure 1.7 Shows a schematic of the Scotch-tape exfoliation steps (K. Novoselov & Neto, 2012). (a) The Scotch Tape is pressed on the 2D material crystals, so few layers of material are attached to the tape. (b, c) detaching the tape from the bulk material and press it against a clean substrate. (d) is the transferred and attached to 2D material on the substrate.

Nevertheless, the disadvantages of this method are the inability to precisely control number of produced layers that results in the combination of monolayers and few layers on the substrate. Also, the contamination resulting from the adhesives will affect directly the charges transport properties. Finally, the sample size is usually too small (on the order of micrometers), which makes it impossible for industrial mass production.

1.6.2 Liquid Phase Exfoliation

Liquid phase exfoliation is an effective method for exfoliating TMDs monolayers. Liquid (chemical) exfoliation peels off layers of 2D material into the solution. The common method of chemical exfoliation used in case of MoS_2 is lithium intercalation (Joensen, Frindt, & Morrison, 1986) (Zhiyuan Zeng et al., 2011). In this method, MoS_2 is treated with many strong reducing reagents containing lithium, MoS_2, for example, $LiBH_4$. $LiMoS_2$ is formed by the intercalation of lithium atoms into bulk MoS_2. Even though bulk MoS_2 does not disperse in water very well compared to $LiMoS_2$. Moreover, nanosheets can be obtained by precipitation or filtration. For bio applications, dispersed MoS_2 with the proper surfactant can be used directly without additional steps (Yang et al., 2014) (Anbazhagan, Wang, Tsai, & Jeng, 2014). However, there are many liquid exfoliation methods do not need strong reagents, and they are called surfactant free methods. In such methods, solvents are carefully chosen as the ones are which minimize the energy of exfoliation are preferred. For example, one of these methods we could obtain nanosheets in three fundamental steps. First we start by mixing MoS_2 powders (or any 2D materials) with the solvent such as isopropanol, with concentrations up to 0.3 mg/mol (Coleman et al., 2011). Then, we proceed by sonicating the solution for about one hour. Finally, centrifuging the produced solution at 500 rpm for 90 min. MoS_2 nanosheets, in this way, are dispersed in the solution that is collected by pipette. This method achieves hybrid films with

enhanced properties. Figure 1.8 shows two types of liquid exfoliation (Coleman et al., 2011) (Eda et al., 2011).

Figure 1.8 Shows the method of liquid exfoliation. (A) MoS_2 Nano sheets in water liquid exfoliation by solution of lithium-intercalation (Eda et al., 2011). (B) The free liquid exfoliation method (top) using the suspension of layered material of thin film obtained from filtration of the solutions in a vacuum (bottom) (Coleman et al., 2011)

Unlike mechanical exfoliation, the number of nanosheets obtained in this method is large. (Eda et al., 2011). In addition, the intercalation method produces a higher yield of MoS_2. However, the used of Li compounds in this process are flammable, for that the process should be done under an inert gas (surfactant free liquid phase exfoliation is insensitive to air). Also, Li is an expensive source, and the material concentration and reaction should be under great control. Finally, the monolayer size is quite small (nanometer size) makes it very difficult for device fabrication.

1.6.3 Chemical Vapor Deposition (CVD)

The Chemical Vapor Deposition (CVD) method is successfully demonstrated and have been used for a long time to grow 2D materials as TMDs. Recording to many published papers, the CVD method was found not to be expensive and not complicated to produce a large area of continuing 2D films.

1.6.3.1 Syntethesis of MoS_2 by (CVD) using $(NH4)_2MoS_4$ as the Precursor

Based on some published scientific reports it found that the CVD method could be used to synthesizes MoS_2 by using thermolysis of ammonium thiomolybdate $[(NH_4)_2MoS_4]$ in a N_2 environment. However, it is known that $(NH_4)_2MoS_4$ leads to MoS_3 formation at different temperatures between 120 and 360 °C (Brito, Ilija, & Hernández, 1995)

1.6.3.2 Synthesis of MoS_2 by (CVD) using S powder and Mo as precursors

The sulfurization of Mo thin films has been used to synthesized MoS_2 layers. The first step was using temperature about 750 °C. Second step consists to expose the Mo film to sulfur vapor to induce a thin MoS_2 layers formation (Zhan, Liu, Najmaei, Ajayan, & Lou, 2012).

CHAPTER II

CHARACTERIZATION AND ANALYSIS TECHNIQUES

For this chapter, we expose the relevant information for the analysis techniques used to characterize the resulting MoS_2 films growth by CVD. For the present work, we used Optical Microscopy (OM), Atomic Force Microscope (AFM), Scanning Electron Microscope (SEM), Energy Dispersive Spectroscopy (EDS), X_ray Photoelectron Spectroscopy (XPS), and Raman Spectroscopy.

2.1 Characterization by Optical Microscopy

Optical Microscopy is used in many areas such as biology, chemistry, physics (Taheri, 2015) and it is useful to get images of different sizes. In this study, the optical microscopy was used systematically after each growth or fabrication steps to see the average morphology of the resulting samples.

2.2 Atomic Force Microscope (AFM)

Atomic Force Microscope (AFM) was invented by Binnig et al. in 1986 (Binnig, Quate, & Gerber, 1986). AFM is an interesting technique it can show different information related to the size and the thickness of the sample. Therefore, it can be used without needed of sample preparation to characterize the surface morphology (figure 2.1). Therefore this kind of technique is great tools for semiconductor material characterization (see figure 2.2). For the present work, by using cross section profiles the AFM was used to see if we have single or mulilayers of MoS_2 after growth. However in this system we faced some challenge to get good AFM images. For this work, we found after the CVD growth that the surface of our samples has many particles on top which make it difficult to find good images.

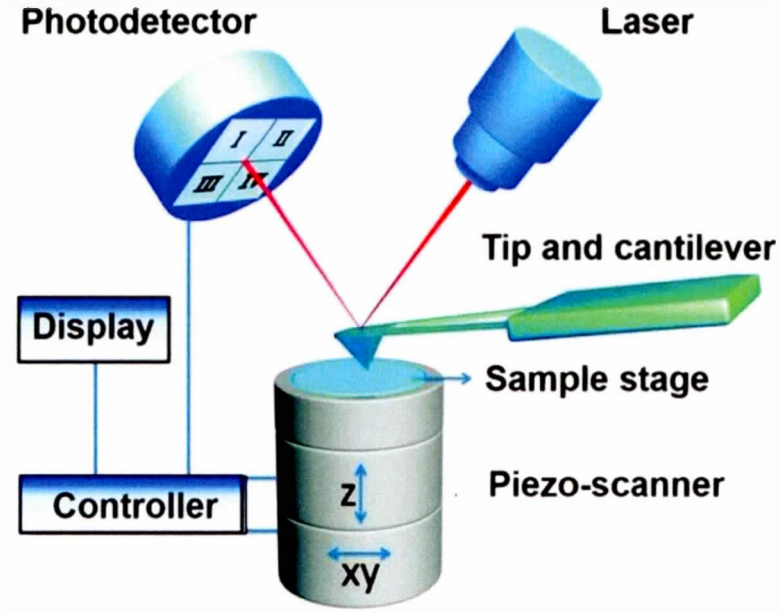

Figure 2.1 The principle of Atomic Force Microscope (AFM) (Zhou, Cai, Tong, & Wang, 2017)

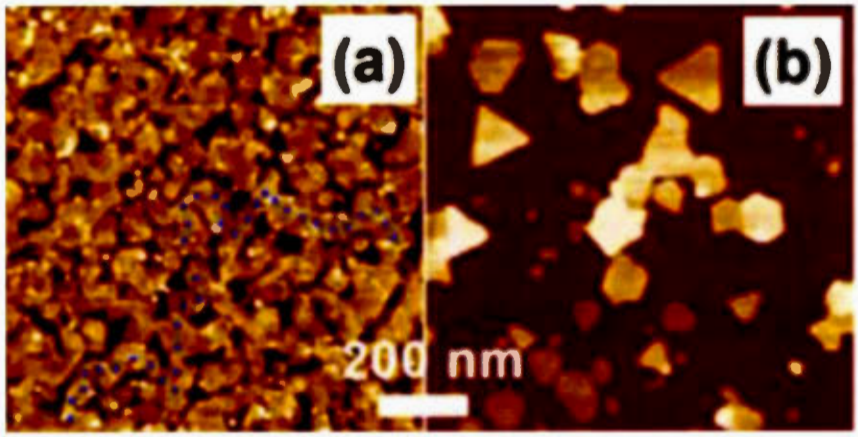

Figure 2.2 AFM images for MoS_2 (H. Liu, Wong, & Chi, 2015)

2.3 Scanning Electron Microscope (SEM)

Scanning Electron Microscope (SEM) is used to get information about the morphology and the composition of the MoS_2 films. SEM works by the magnification of an electron beam, which is produced by a source gun (see Figure 2.3). There are one or two condenser lenses that focus the beam after being accelerated towards the anode. The beam is deflected in x and y directions, by pairs of scanning coils, allowing scanning in a raster mode over a rectangular area of the sample surface. There are various detectors capture the emissions that produced from the interaction between the electron beam and specimen. Backscattered electrons and secondary electrons are specific types of emitted electrons provide compositional information and morphological topological-contrast, respectively. Using an X-ray detector provides further compositional information (Suga et al., 2014) (Reithmeier, Vynnyk, & Schultheis, 2010). Thus, SEM can show information about the surface and further characterize the size of microstructures for the triangle image for MoS_2 monolayer (see Figure 2.4).

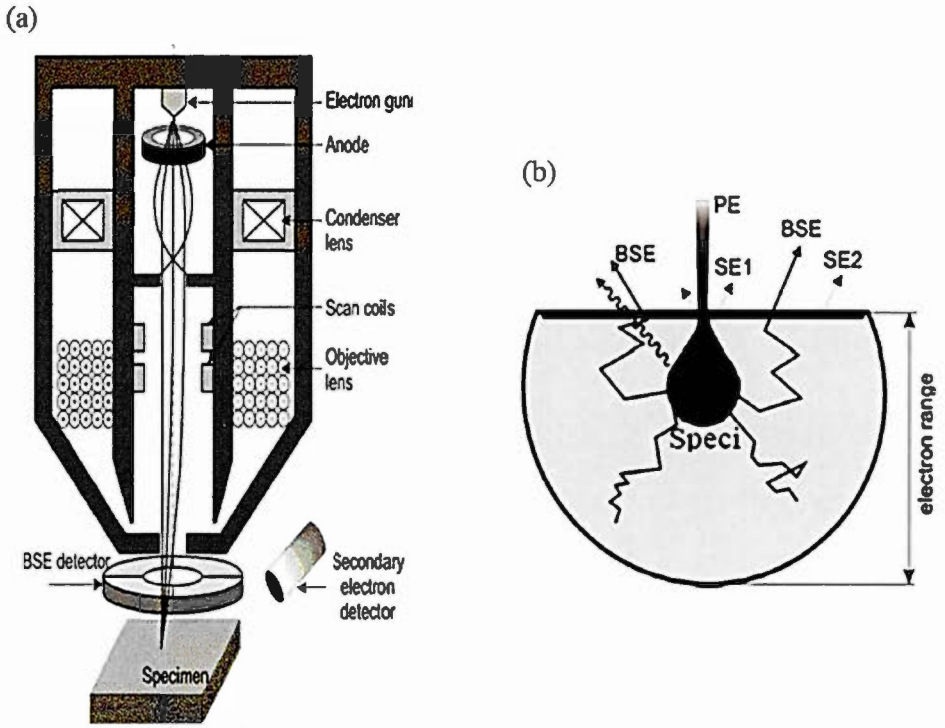

Figure 2.3 Basic photograph of (a) Schematic diagram of SEM, (b) introduction volume (Reithmeier et al., 2010)

SEM is one of the most used techniques for 2D materials characterization in which we can an average idea for the resulting product. For instance, Figure 2.4 exhibiting the high resolution SEM image for MoS_2. (Sheu, 2015)

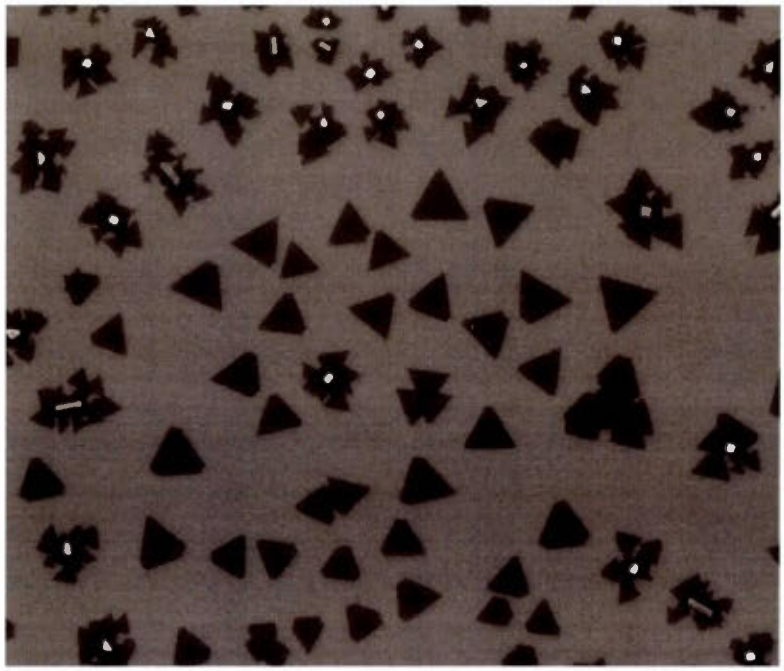

Figure 2.4 SEM image with Higher magnification scan of MoS_2 (Sheu, 2015)

2.4 Energy Dispersive Spectroscopy (EDS)

Energy Dispersive Spectroscopy (EDS) is a chemical analysis technique used to determine the concentration of most elemental species in a given sample. The fundamental principle of this method is the emission and detection of x-rays from a given sampling volume that are characteristic to specific elements (Goldstein et al., 2003). A material can produce x-rays when bombarded with high-energy electrons. The X-ray generation process (Figure 2.5) is initiated with ejection of an inner shell electron forming a vacancy. As a result of this excited state, an electron jumps from the outer shell into the vacant site filling the inner shell. During this process, the sample

fluoresces X-ray of energy which is equal to the energy difference between the initial state and the final state. Since each atom possesses its unique and discretized energy levels, the x-Ray fluorescence is characteristic and distinctive to that atom as well. The initial nomenclature is obtained from electronic shell of the initial vacancy that created by the electron using K, L, M and N as shell name. These letters indicate the number of shells above the vacancy from which replacing electron as shown in Figure 2.5. The output for EDS analysis is a plot of intensity or x-ray counts vs. characteristic energy in electron volts (eV). EDS is a useful technique to detect possible pathological deposition of materials.(Scimeca, Bischetti, Lamsira, Bonfiglio, & Bonanno, 2018)

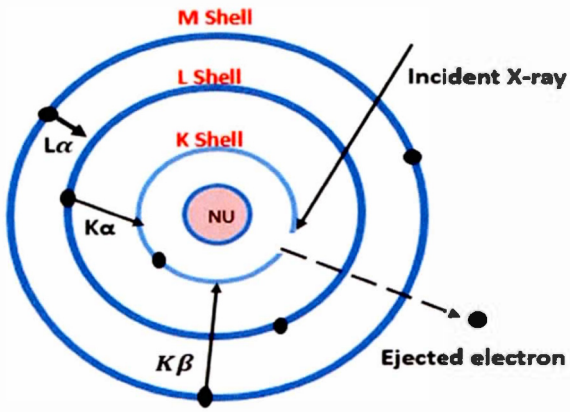

Figure 2.5 The Energy Dispersive X-ray Microanalysis (EDX shown leaving electron) (D.Sharata ,2018)

2.5 Raman Spectroscopy

Raman spectroscopy is a quick method to get structural and chemical information at the microscale level without sample preparation (see Figure 2.6). The Raman effect is considered as an inelastic light scattering process. It is known that when a substance is exposed to a strong light source (laser), most of the energy will be scattered elastically. The most intensive scattering is Rayleigh scattering, happens when the electron could relax with no nuclear movement. This an elastic process does not result in any appreciable changes in energy. On the other hand, Raman scattering is a much rarer event, contributes to one in 10^6–10^{10} of the photons scattered, and it occurs when the interaction between electrons and light takes place, and the nuclei begin to move at the same moment. There are appreciable changes in energy of the molecule as a result of the fact that the nuclei are much heavier than the electrons. Change in energy is either to lower or to higher energy based on whether the process starts from a molecule in a vibrational excited state (anti-Stokes scattering), or from a molecule in the ground state (Stokes scattering) (see Figure 2.7), [(Smith & Dent, 2005), (Edwards & Chalmers, 2005).

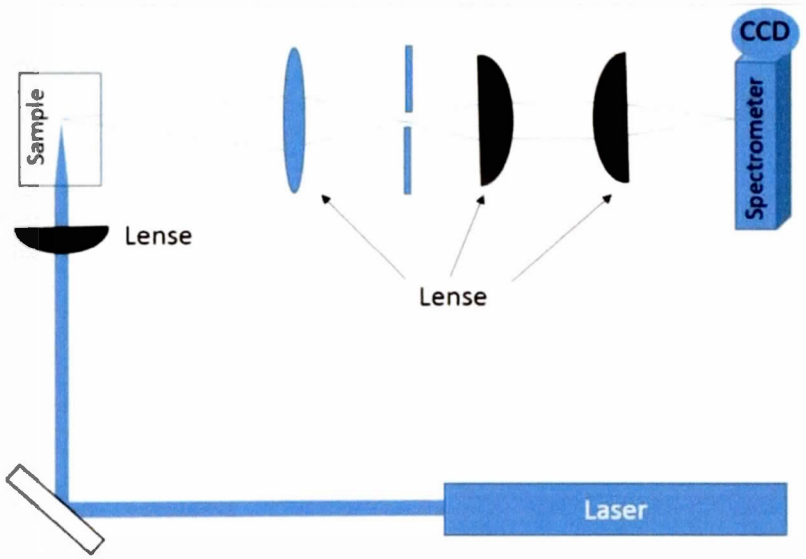

Figure 2.6 Raman configuration system (Taheri, 2015)

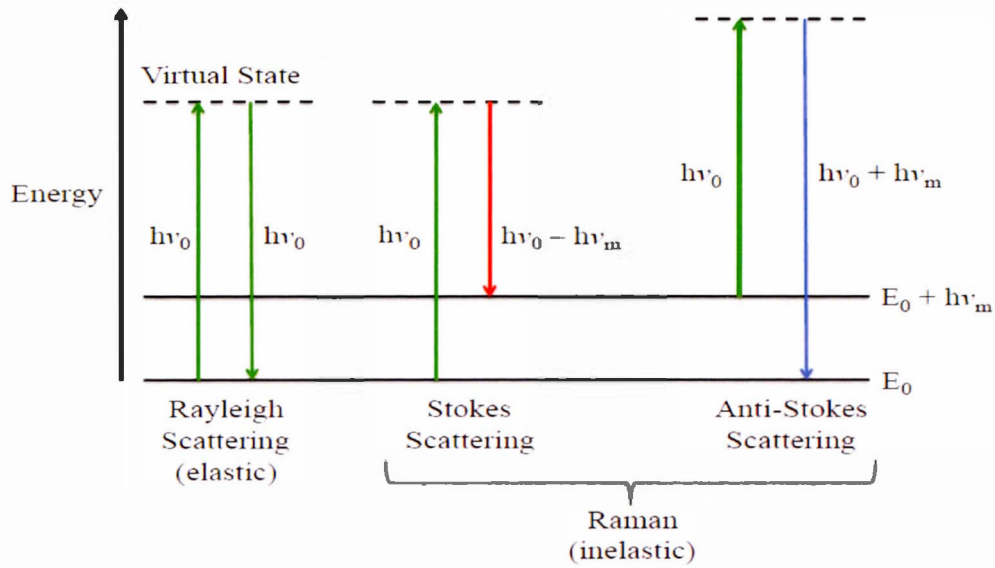

Figure 2.7 Shown the energy level and Raman scattering and Rayleigh scattering process (Smith & Dent, 2013)

2.6 X-ray photoemission spectroscopy

The XPS is a sensitive technique used to get information about the chemical bonding structure of MoS_2 monolayer (Figure 3). The XPS binding energies of Mo 3d and S 2p peaks are 232.4 eV and 235.5 eV, respectively. For the present work, the chemical composition of the modified MoS_2 film surfaces is studied systematically by XPS. As shown in chapter 4, results and discussion (Figures 4.15 and 4.16) this technique is used to understand the transformations that occur on the surfaces under different growth conditions by showing the changes of the chemical bonding. (Actis et al., 2008)

2.7 Photoluminescence (PL)

Photoluminescence (PL) for MoS_2 (Steinhoff et al., 2015) shows weak bonding of Van der Waals forces sheets with a strong indirect band gap around 1.85 eV. The PL it has been used for many applications and it very useful of the photocatalytic and electronic structure. MoS_2 thin film has great optical properties. The optical band gap of MoS_2 showed a clear dependence on the MoS_2 film thickness, with thinner films having a larger band gap energy. These results are consistent with theory and observations made on MoS_2 flakes prepared by different methods. For this study, we used an excitation laser 532 nm with a peak position of direct band gaps around 1.85 eV to get PL mapping of MoS_2 monolayer.

CHAPTER III

MoS_2 SYNTHESIS BY CHEMICAL VAPOUR DEPOSITION (CVD) AND CHARACTERIZATION

3.1 CVD system configuration

Chemical Vapour Deposition (CVD) is a materials growth method in which the gaseous reactants undergo dissociation and chemical reactions while the environment is activated by heat, light or plasma. This result in the formation of stable solid products on top of a substrat or a catalyst. The CVD is the most efficient method for continuous monolayer transition metals dichalcogenides growth.The CVD technique allows a good scalability as well as low-cost for TDMs growth. It has been shown that the quality of the resulting MoS_2 film by CVD could be useful optically and exhibiting excellent device properties (see Figure 3.1).

In this study, we used two furnaces to control the temperature during the growth. The furnaces are equipped with a temperature controller and a programmable digital model enables the operator to program up to different ramp segments (heat-up or cool-down rate) (Choy, 2003). Sulfur powder was placed on the first furnace at low temperature and the MoO_3 precursor were placed in the second one at high temperature (see Figure 3.2). Compared to several research reports on MoS_2 growth, using one furnace is quite complicated to control both temperature plateau, one for MoO_3 and the seconde for S at the same time. The advantage of using CVD is that we can grow a large area of MoS_2 (counting film). In addition, we can control the time for growth and the temperature for both furnaces.

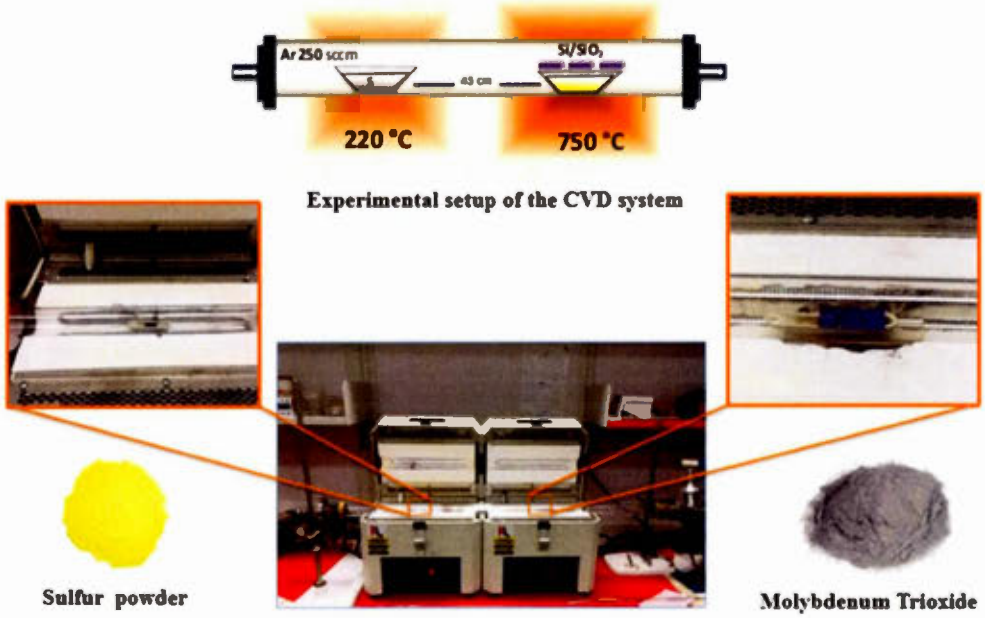

Figure 3.1 CVD system steps used to grow a MoS_2 films on top of SiO_2/Si substrates by reacting S and MoO_3 powders in CVD furnaces (D.Sharata, 2017 Siaj Lab)

Prior to all, in this study, first we used one furnace to grow MoS_2. However, as we can see from the optical microscopy images, we did not succeed in getting continuous MoS_2 layers by using one furnace (see Figures 3.3 and 3.4)

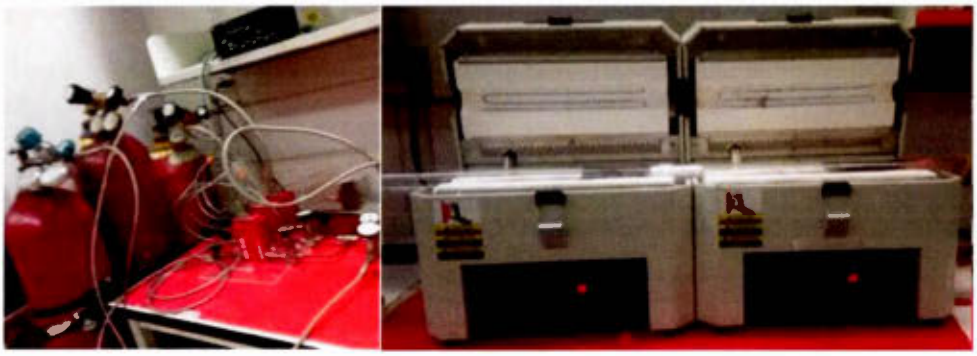

Figure 3.2 The Chemical Vapour Deposition (CVD) system in Siaj's laboratory (D.Sharata, 2017 Siaj lab)

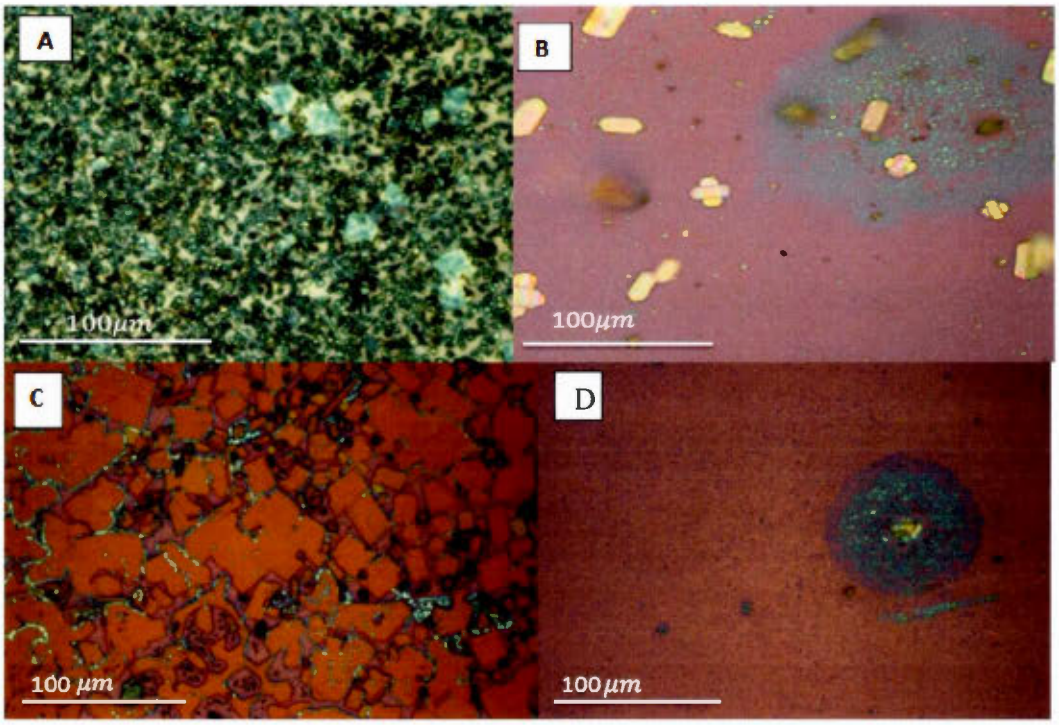

Figure 3.3 Optical microscope images show MoS_2 morphology resulting from the growth process by suing only one furnace

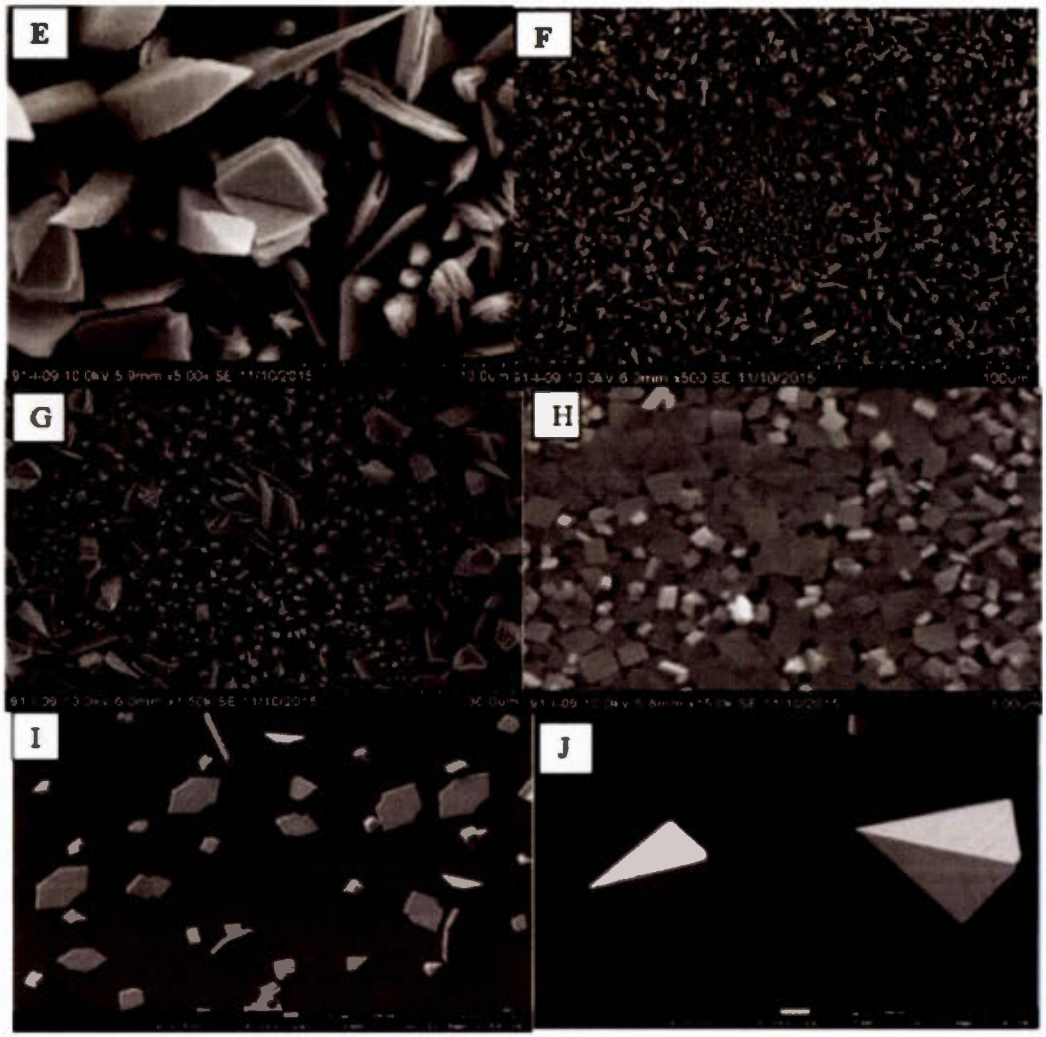

Figure 3.4 SEM images show the effect of the time used (duration) for growth of MoS_2 by using one furnace as CVD system

3.2 Growth Mechanism

During the sulfidation of molybdenum oxide (MoO_3) into MoS_2 nanocrystals the oxide precursor undergoes two overall reactions, i.e., the reduction of Mo(VI) to Mo(IV) and the sulfidation of MoO_3 to MoS_x. As shown schematically in Figure 3.5, these reactions can occur simultaneously.

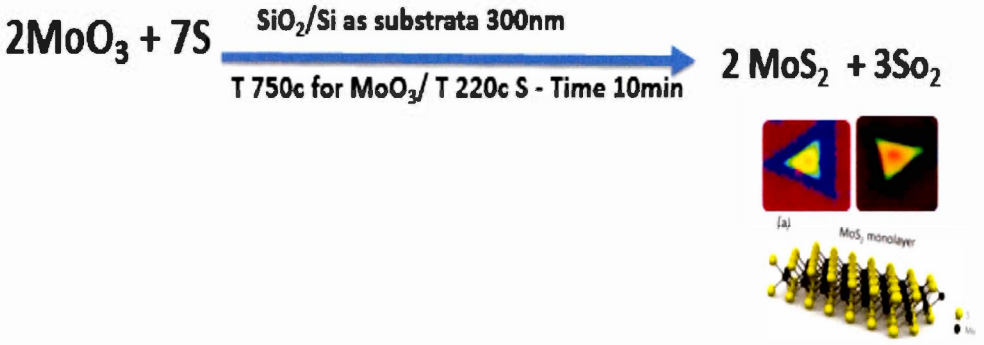

Figure 3.5 The chemical reaction of MoS_2 (Feng et al., 2015)

3.3 Sample preparation

We used SiO_2/Si (300 nm of SiO_2 on top of Si) as substrate for the MoS_2 growth and devices fabrication. First, we cut the SiO_2/Si wafer to many pieces (1 cm^2 each), and under sonication, we clean all substrates with H_2SO_4 and H_2O_2 ; 3:1 solution for 15 minutes. Next, we clean three times the SiO_2/Si substrate by DI water. Finally, all substrates are dropped in isopropanol (IPA) solution to remove the water. This cleaning method gives the best result for MoS_2 triangle growth.

3.4 MoS_2 growth strategy in the present work

The sulfur powder (S), 0.2 g (99.5%, Sigma-Aldrich) and molybdenum trioxide (MoO_3), 0.3 g (99%, Sigma-Aldrich) powder were used as the S and Mo precursors, respectively (Lee et al., 2012). During the growth time, 250 sccm of argon (Ar) was used as the carrier gas. As we mentioned above, we used two furnaces for the growth, one is used for S and one for MoO_3. The S powder introduction to the second furnace could be accomplished at a temperature range between 120 °C to 290 °C. The growth substrate was placed face down to the boat with containing MoO_3 powder in the second furnace . The boat was located at the center of the fused quartz tube. The second furnace temperature was raised from 650 °C to 750 °C for MoO_3 for 40 minutes. The temperature in the second furnace was kept stable at 750 °C for 10 minutes. After the growth step, the furnaces were left at room temperature to cool down. The samples were taken off from the quartz tube and as we can see from the images obtained from this experiment that the conditions mentioned above are the best conditions for the MoS_2 growth by CVD method (see Figure 4.3 in results section) .

CHAPTER IV

DISCUSSION AND RESULTS

This chapter will present the results of growing MoS_2 monolayer domains as well as counting MoS_2 film.

4.1 The temperature effect on MoS_2 growth

The temperature effect on the MoS_2 growth morphology can be visualized directly by the optical microscopy (see Figure 4.1). In this study, we used different growth temperatures starting from 650 °C to 800 °C (650 °C, 700 °C, 750 °C and 800 °C). We found that the best condition to get high quality MoS_2 was at 750 °C for 10 minutes reaction. For each reaction, the temperature was increased gradually every 3 minutes until reaching the desired temperature. After that we keep the furnace at the growth temperature (650 °C, 700 °C, 750 °C and 800 °C) for 40 minutes. The growth of MoS_2 needs slow steps to allow enough time for S to react with MoO_3. As we mentioned above, using two furnaces to control the temperature of S and for MoO_3 is the best condition for the MoS_2 growth.

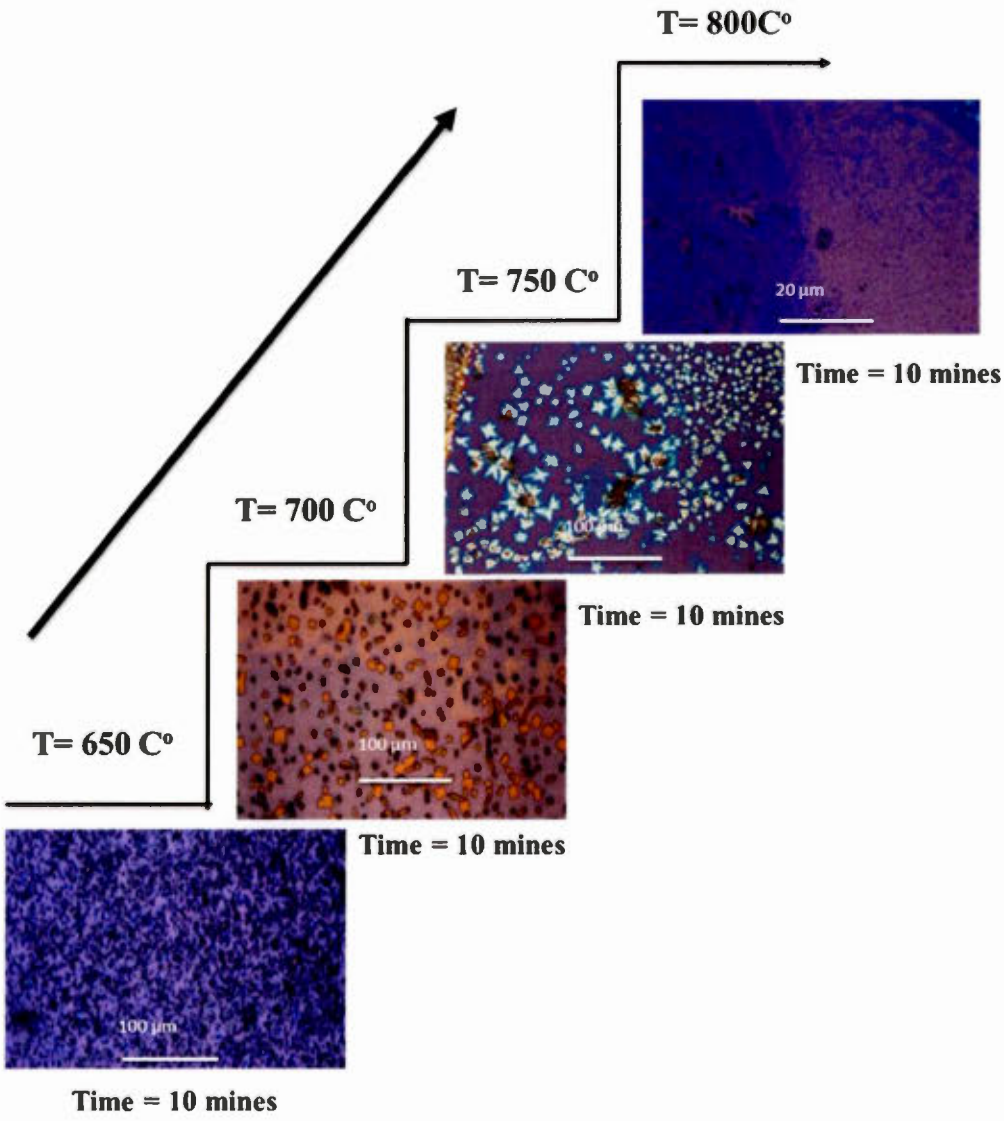

Figure 4.1 Optical microscopy images show the temperatures effect on MoS_2 domains growth by CVD on top of SiO_2/Si

4.2 The effect of Ar gas

Prior to any growth reaction, we used 100 sccm of Ar gas during 10 to 15 minutes to clean CVD systems. For the growth, as carrier gas, we used different flow rates of Ar: 250 sccm, 180 sccm 100 sccm, and 80 sccm. We found a significant difference on the morphology of the produced materials by changing the carrier gas flow rates between 80 sccm and 180 sccm. Indeed, we found that the flow rate should be more than 250 sccm. High carrier gas flow rates seem to help the reaction between S and MoO_3 to grow a high amount of MoS_2 (see Figure 4.2).

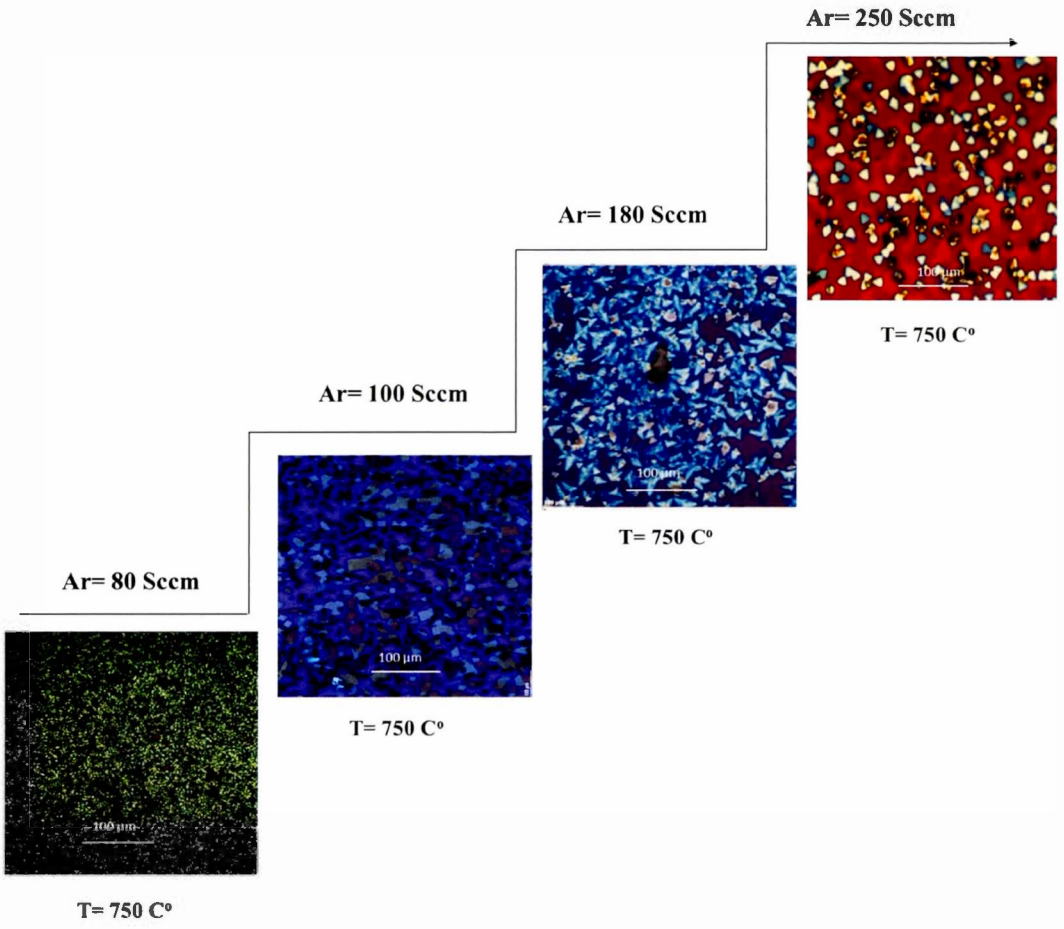

Figure 4.2 Effect of Ar gas on the growth of MoS_2 at constant temperature

4.3 The morphology of MoS_2 samples by Optical microscope

The optical microscopy was used systematically after each growth or fabrication step to see the average morphology and the scale of the resulting samples. Figures 4.3a, 4.3b and 4.3c show an average distribution of MoS_2 flakes with different size and shape (tringle). Figures 4.3c shows the MoS_2 heterostructures as well as the different layers in the center of triangular structure.

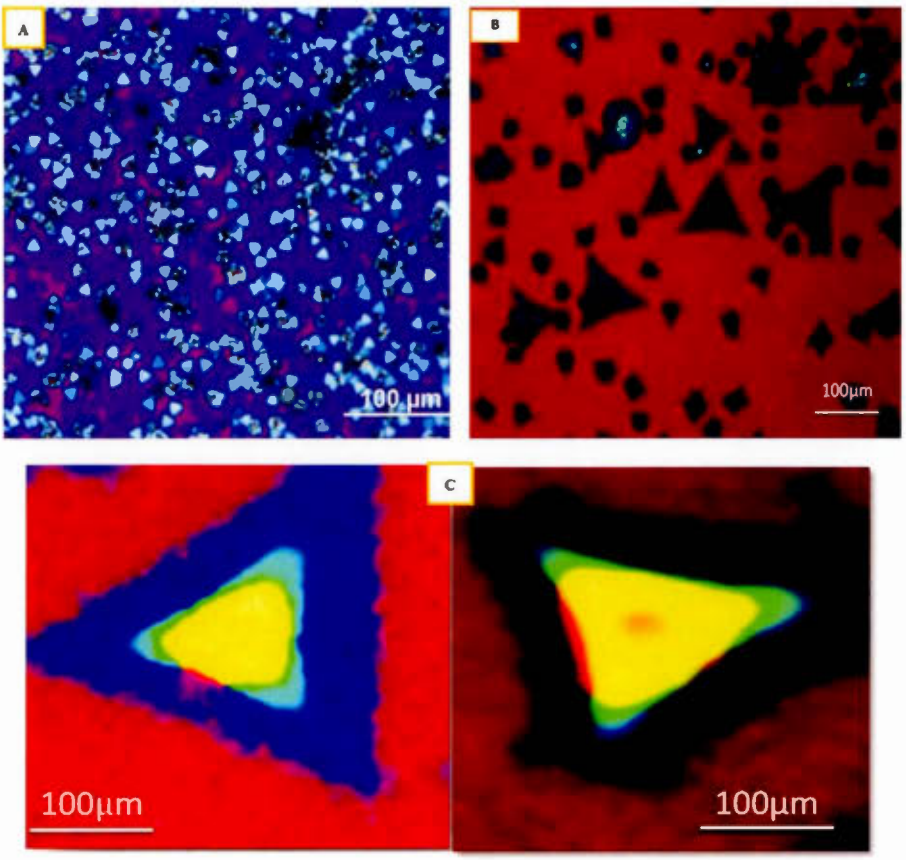

Figure 4.3 Optical images of MoS_2 flakes on top of silicon substrate (A) triangular shape of MoS_2 and a continuous film. (B) Monolayer triangle MoS_2 flakes (C) MoS_2 triangles heterostructures with different layers

4.4 Scanning Electron Microscope (SEM)

A Scanning Electron Microscope (SEM) has been used for the MoS_2 morphology characterization. The SEM gives information about the surface morphology and the size of MoS_2 monolayer microstructures. Figures 4.4 and 4.6 show a typical MoS_2 single layer images of the flower-like crystalline structures including the nucleation in the center of triangles with different sizes increase from 1μm to 10μm. We found that the nucleation density increase by increasing the reactant concentration and growth time. We found that the large triangle growth start with simple nucleation in the center (H.-J. Xu et al., 2017). Figure 4.5 exhibits SEM images of monolayer triangular islands at 750 °C.

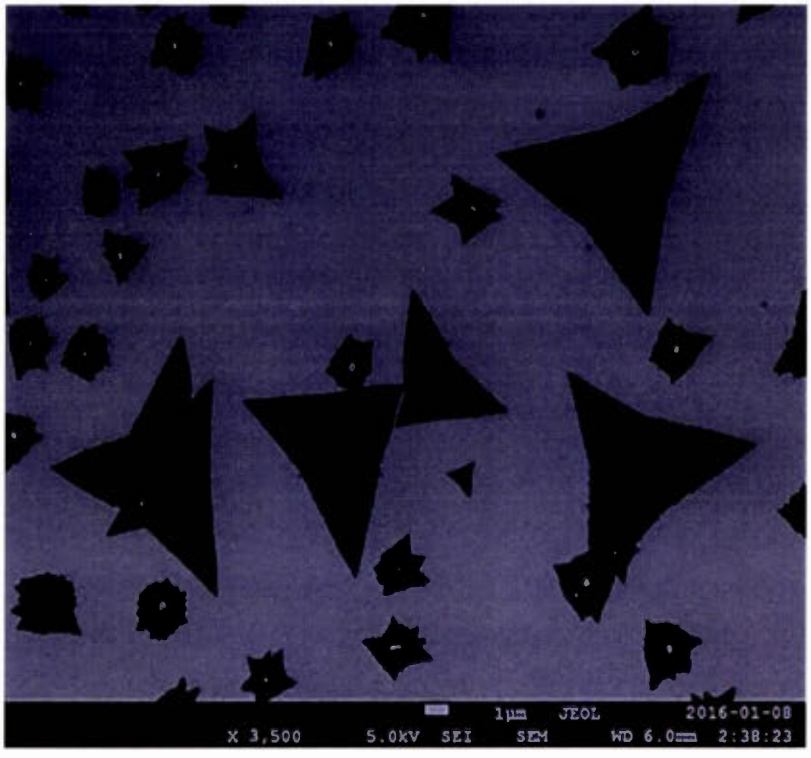

Figure 4.4 SEM image of MoS_2 shows triangle flake formation with flower-like crystalline structure and nucleation in the center

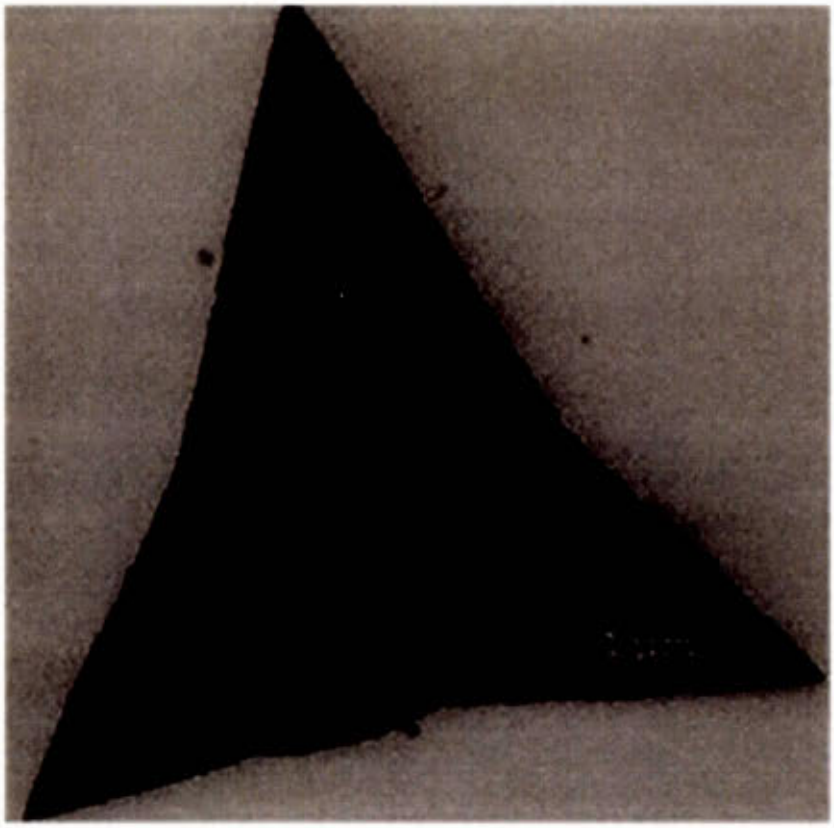

Figure 4.5 SEM high topographical resolution images of a MoS_2 triangle single crystal

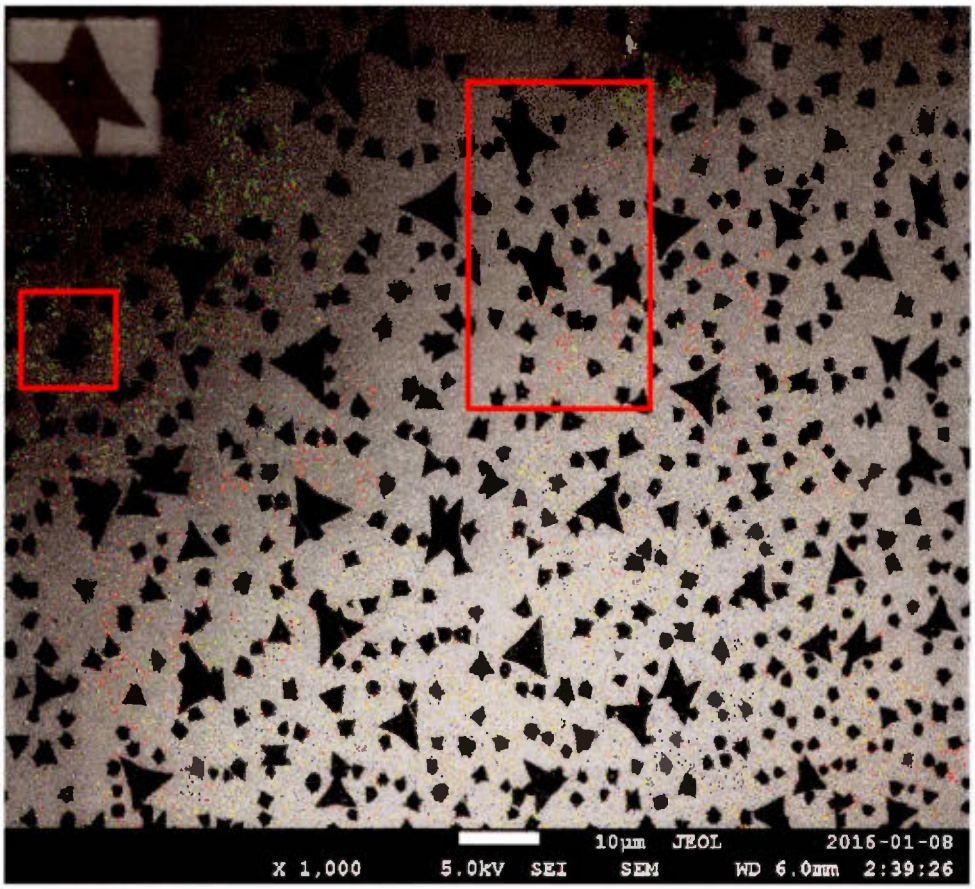

Figure 4.6 Large scale SEM image of MoS_2 flakes

4.5 Energy Dispersive Spectroscopy (EDS)

Energy Dispersive Spectroscopy, also called Energy Dispersive X-ray Microanalysis (EDX), works together with Scanning Electron Microscope to provide interesting information on the chemical analysis.

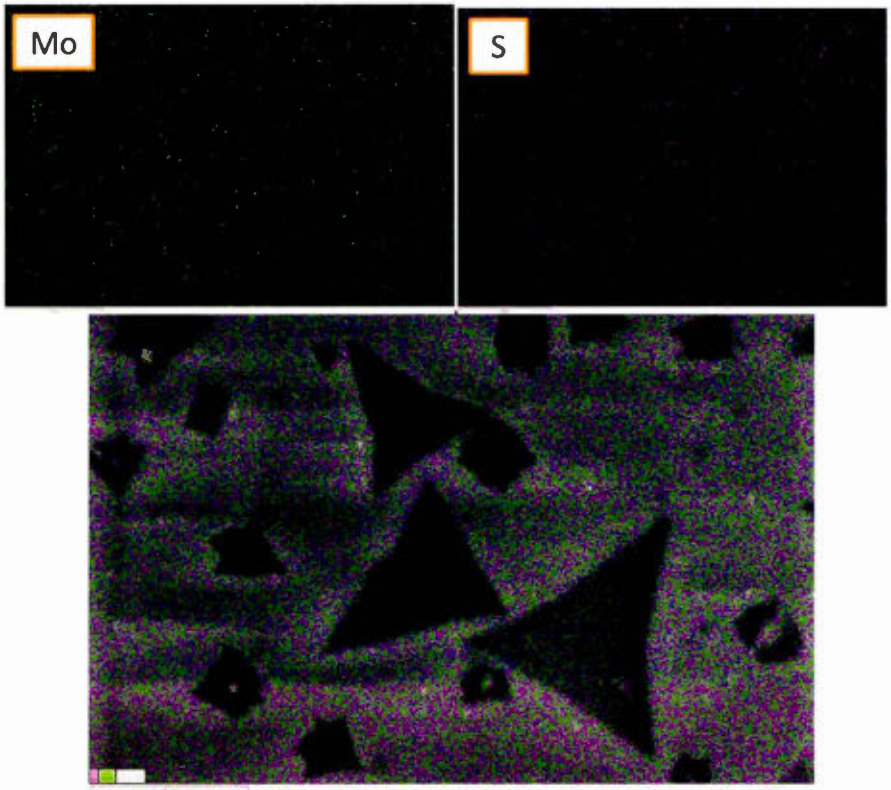

Figure 4.7 EDS mapping of triangular Mo, S on MoS_2.

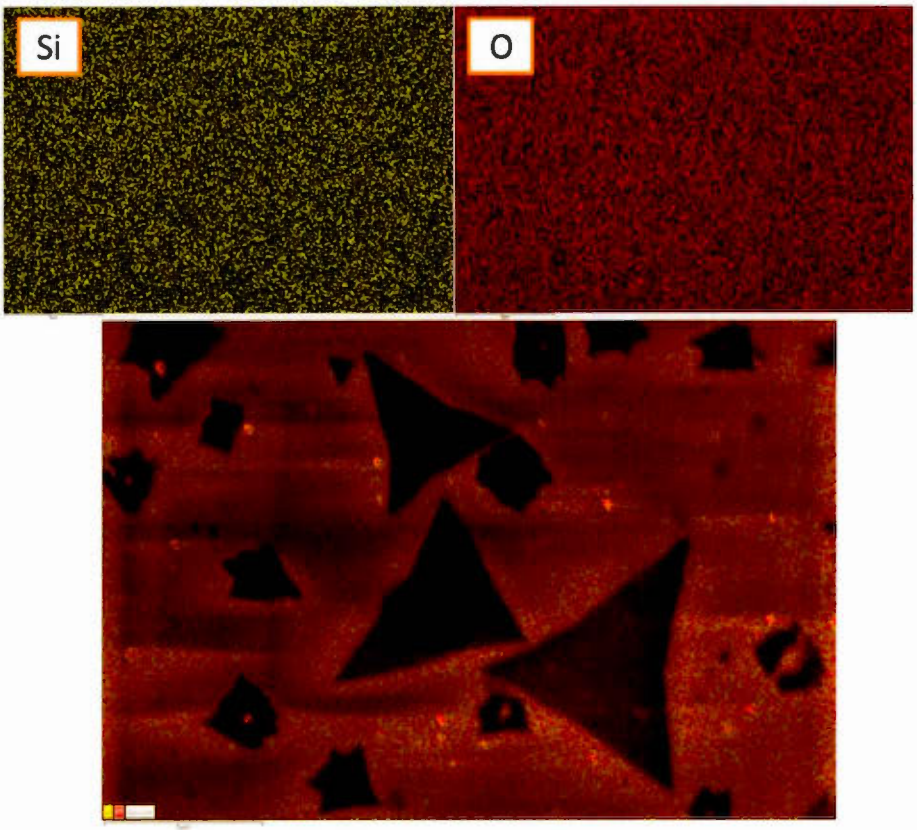

Figure 4.8 EDS mapping of Si and O elements on triangular MoS_2

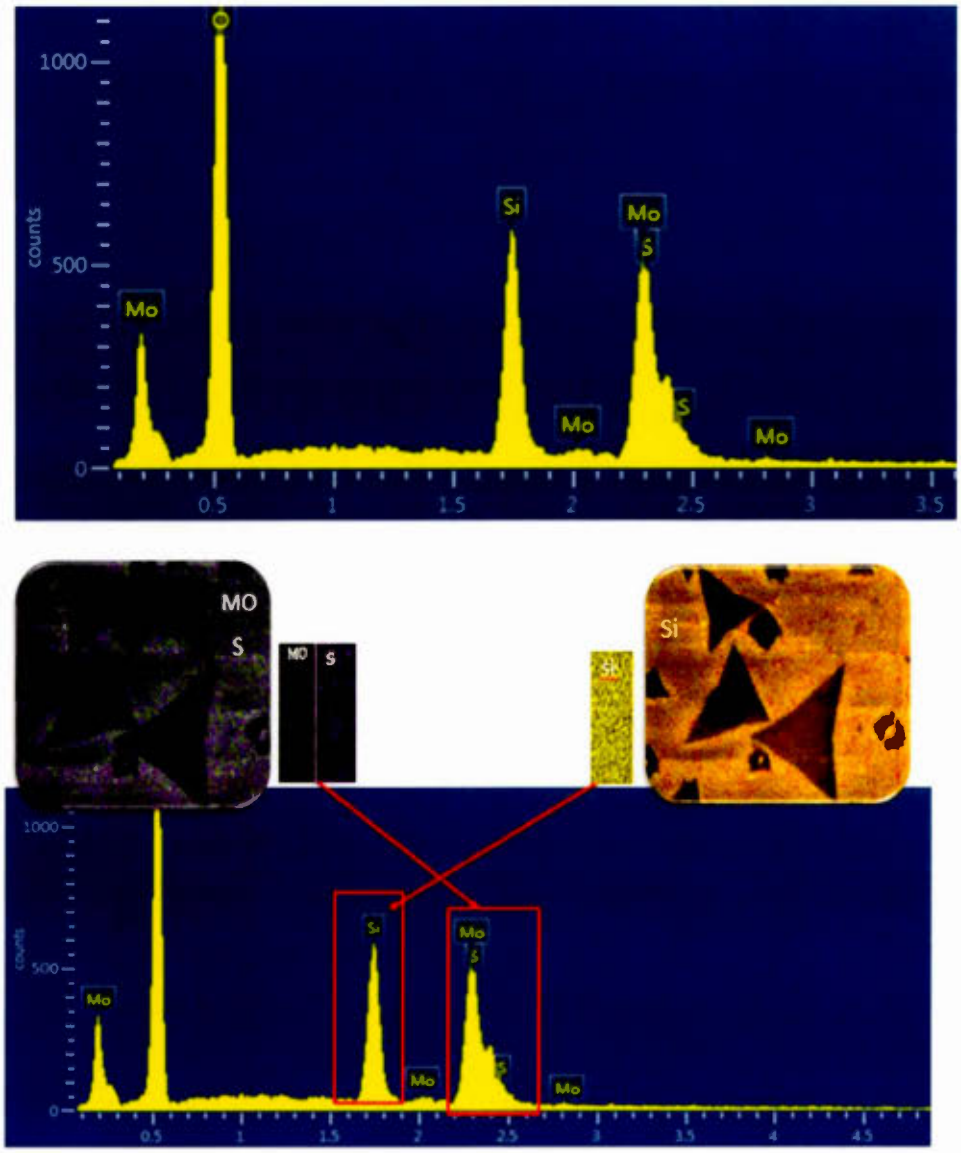

Figure 4.9 EDS spectrum of MoS_2 and the EDS mapping of Mo, Si, S and O of MoS_2. The output for EDS analysis (a plot of intensity or x-ray counts vs. characteristic energy in electron volts (eV)) showing K peaks of Mo, Si, S and O

4.6 Atomic Force Microscopy (AFM)

Atomic Force Microscopy (AFM) is the most common type of scanning probe microscopy. It is used to image a topographical surface, determine the roughness of the surface, and measure the thickness of a MoS_2 layer. AFM has been used for 2D material such as graphene (Zheng et al., 2012) ,(Stankovich et al., 2007)

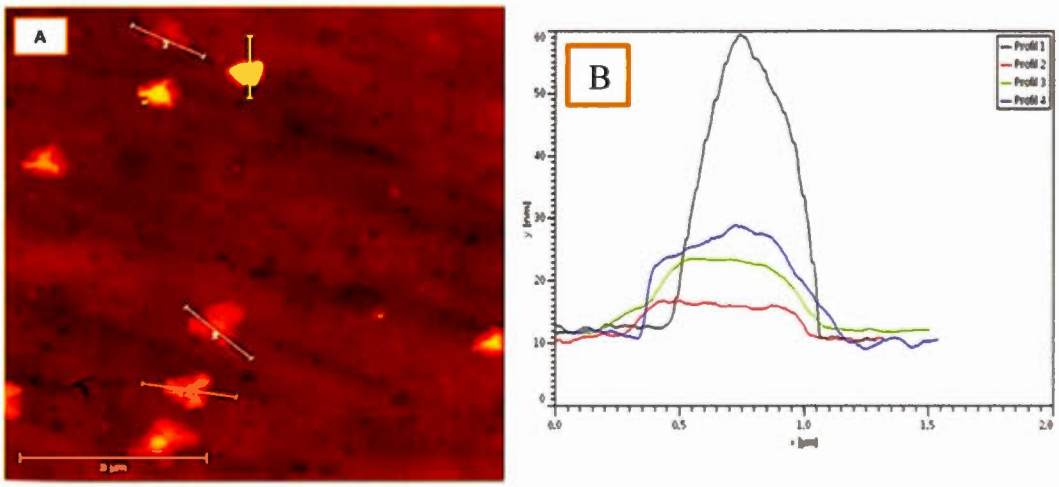

Figure 4.10 (A) AFM image of triangular structures of MoS_2. (B) High profile of different samples

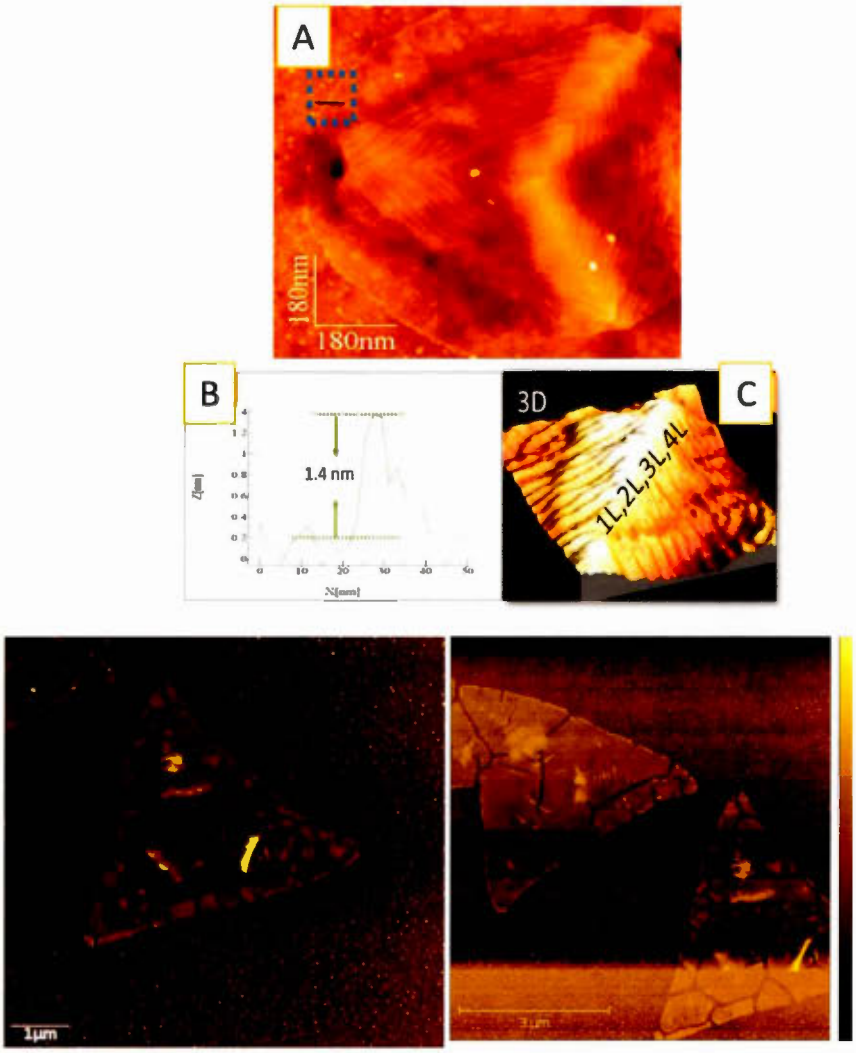

Figure 4.11 A) High-resolution AFM image of MoS_2. B) AFM section profile along the line in the panel (A) (MoS_2 thin layer thickness around 1.4 nm). C) 3D image of the panel (A). D) AFM topography map shows triangles of MoS_2 with some defect

4.7 Raman Spectroscopy

Raman spectroscopy is an easy and quick method to get structural and chemical information at the molecular level with minimum sample preparation. In this study, we performed Raman mapping by using laser with 532 nm excitation wavelength. By using Raman, there are two types of vibrational modes in MoS_2 (Intralayer and interlayer modes). The interlayer modes are related to the chemical composition of a layer (or layers) and are their fingerprint. These modes can be slightly influenced by the number of layers. However, the interlayer modes, due to the high mass of the layers, are observed at very low frequencies and their position depends on the number of layers. As a result, both types of modes can be used to determine the number of layers. The number of layers can be found by determining the distance between two fingerprint peaks (observed at ~383 cm^{-1} and ~408 cm^{-1}) in bulk MoS_2. With increasing numbers of single layers the mode at (~383 cm^{-1}) shifts to lower frequencies and the mode at (~408 cm^{-1}) shifts to higher frequencies. These two peaks correspond to E_{2g} (383.6 cm^{-1}) and A_{1g} (405.6 cm^{-1}), (see. Figure 4.12).

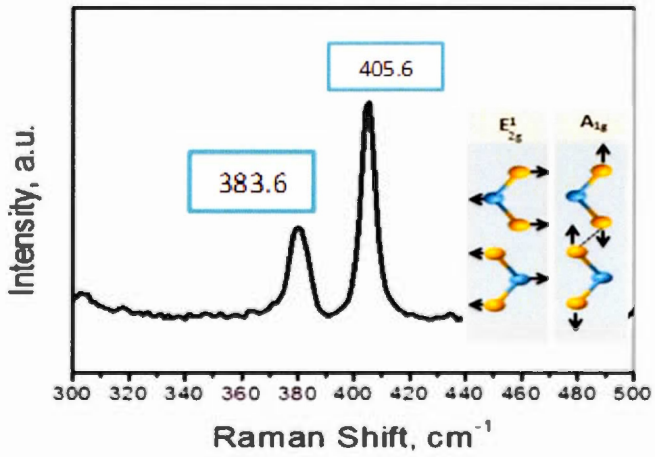

Figure 4.12 Raman spectra of MoS_2 in the fingerprint region

Like graphene, single-layer and few-layer molybdenum disulfide has distinctive signatures in its Raman spectrum. For that to show clearly that we have succeeded in

our MoS_2 CVD growth, we did different Raman measurements in several areas of our samples (See figures 4.13a and b). The analysis is very straightforward and consists of mapping individual regions found opticaly (figure 4.13a). As the Raman spectra are relatively well resolved (Figure 4.13b), we can conclude that we have a continuous MoS_2 film (spectrum A) and multilayer in the triangle region (spectrum B, C, D and E).

The Raman spectrum of bulk MoS_2 has two prominent peaks: an in-plane (E_{2g}) mode located around (383 cm^{-1})and an out-of-plane (A_{1g}) mode which is located at (407 cm^{-1}). The in-plane mode corresponds to the sulphur atoms vibrating in one direction and the Molybdenum atom in the other, while the out-of-plane mode is a mode of just sulphur atoms vibrating out-of-plane. As MoS_2 becomes single-layer these two modes evolve with thickness. The in-plane mode upshifts to (386 cm^{-1}) and the out-of-plane downshifts to (404 cm^{-1}). The difference of these two modes (~18 cm^{-1}) can be used as a reliable identification for monolayer MoS_2.

For the present work, the spectrum shows different peaks very characteristic of monolayer formation, which is in agreement with the literature. The Raman spectrum exhibits one peak at (383.6 cm^{-1})and another peak at (408.6 cm^{-1}). These two peaks correspond to E_{2g} (383.6 cm^{-1}) and A_{1g} (408.6 cm^{-1}) as we can see triangles of MoS_2 with different sizes. Figures 4.12 shows the Raman mapping of MoS_2 films.

In addition to Raman spectroscopy, we performed nanoscale confocal photoluminescence (PL) in different regions of the resulting MoS_2 materails (see Figure 4.14a). The PL spectrum of MoS_2 shows a strong photoluminescence signal indicating an indirect to direct bandgap transition (see Figure 4.14a).

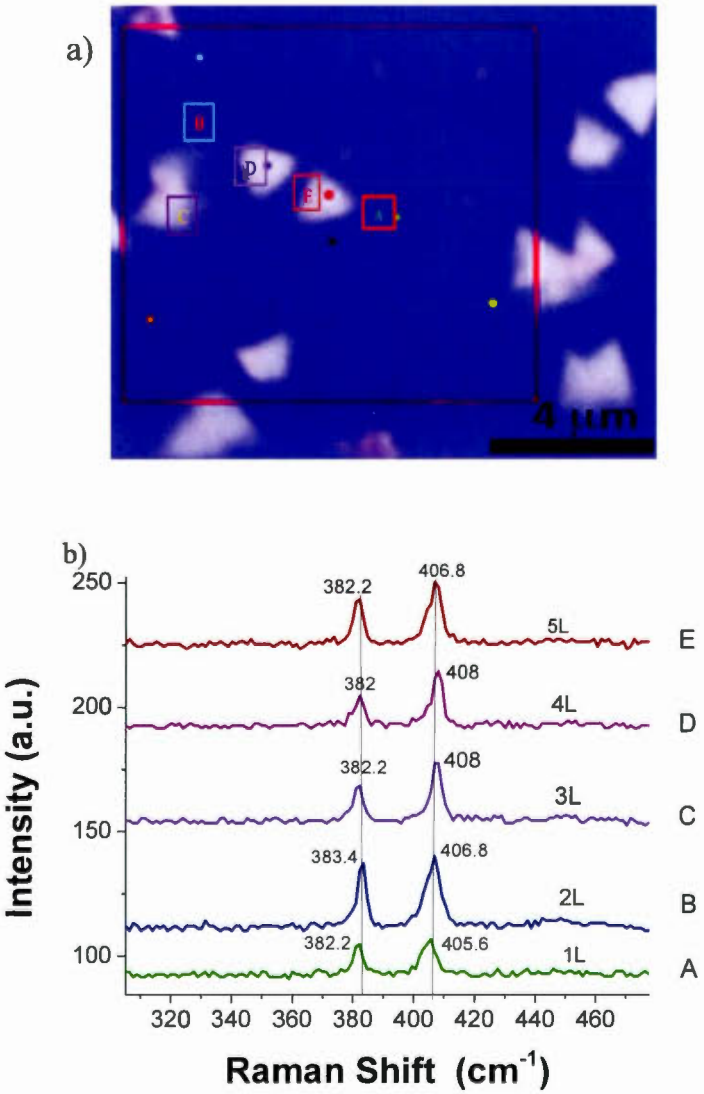

Figure 4.13 a) Optical image for a typical MoS_2 film growth. b) Raman spectra in different areas shows clearly layer dependent MoS_2 Raman spectroscopy

4.8 Photoluminescence (PL)

MoS_2 is a semiconductor with direct band gap around 1.85 eV. MoS_2 thin film has great optical properties (Steinhoff et al., 2015) and many applications in photocatalytic (Gourmelon et al., 1997; Ho, Yu, Lin, Yu, & Li, 2004)

The thin-layered TMDs, as novel two-dimensional materials, undergo remarkable changes in their electronic structures depending on the number of layers from indirect-band-gap bulk semiconductors to direct-band-gap monolayer semiconductors (Eda et al., 2011). In the present work we have a great photoluminescence spectrum of MoS_2 with direct band gaps about 1.85 eV (see Figure 4.14 a).

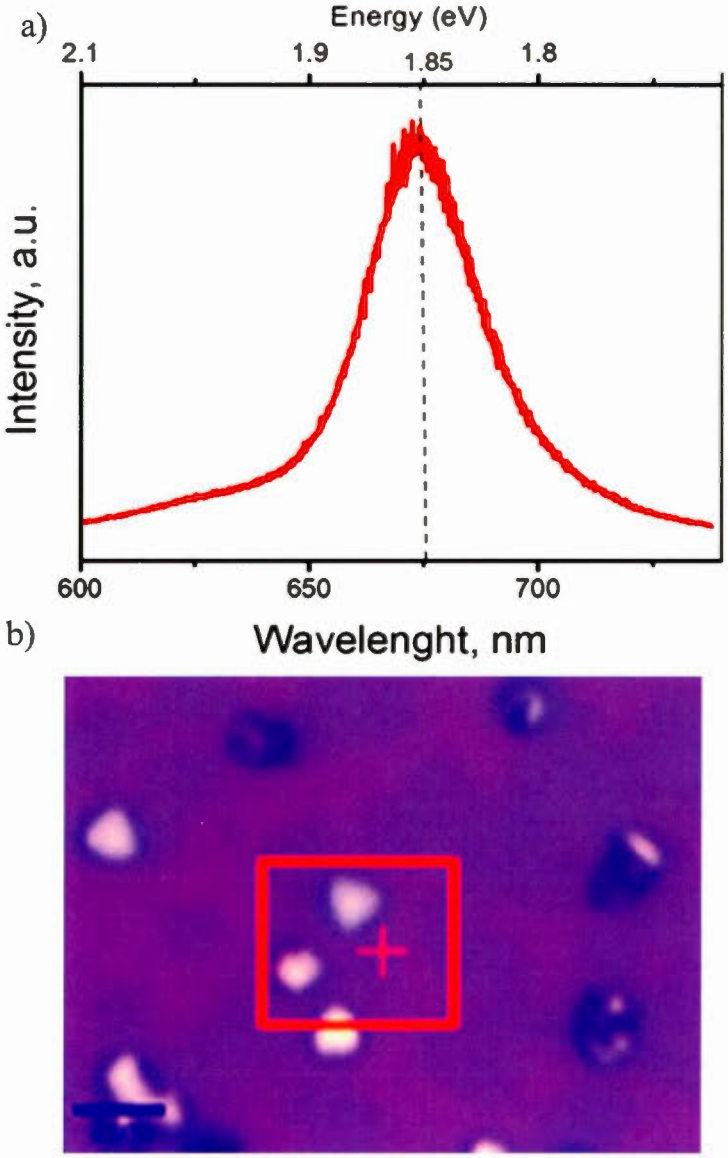

Figure 4.14 a) Shows a typical photoluminescence spectrum of MoS_2 with a direct band gap at about 1.85 eV. b) optical image of the MoS_2 film.

4.9 X-ray photoemission spectroscopy

X-ray photoemission spectroscopy was used for MoS_2 characterization (Actis et al., 2008). An XPS survey scan gives useful information on which elements are present at the surface. Molybdenum disulfide was analyzed using high-resolution X-ray photoelectron spectroscopy (XPS). High resolution of molybdenum (Mo $3d_{5/2}$ and Mo $3d_{3/2}$) and Sulfur ($S_2p_{1/2}$, $Sp_{2\ 3/2}$) XPS data for the produced MoS_2 films are presented in Figure 4.15 and Figure 4.16. The high-resolution spectrum of molybdenum (Mo $3d_{5/2}$ and Mo $3d_{3/2}$) displays two peaks located at 229.2 eV and 232.6 eV, respectively and the high-resolution spectrum of sulfur ($S_2p_{1/2}$, $Sp_{2\ 3/2}$) with two peaks located 163.6 and 162.8 eV, respectively.

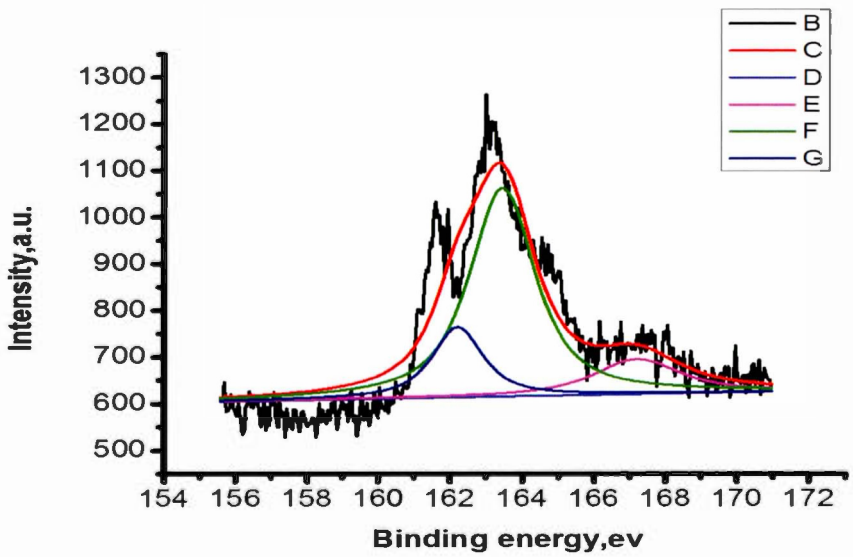

Figure 4.15 Fitted high resolution S 2p XPS peak for MoS_2

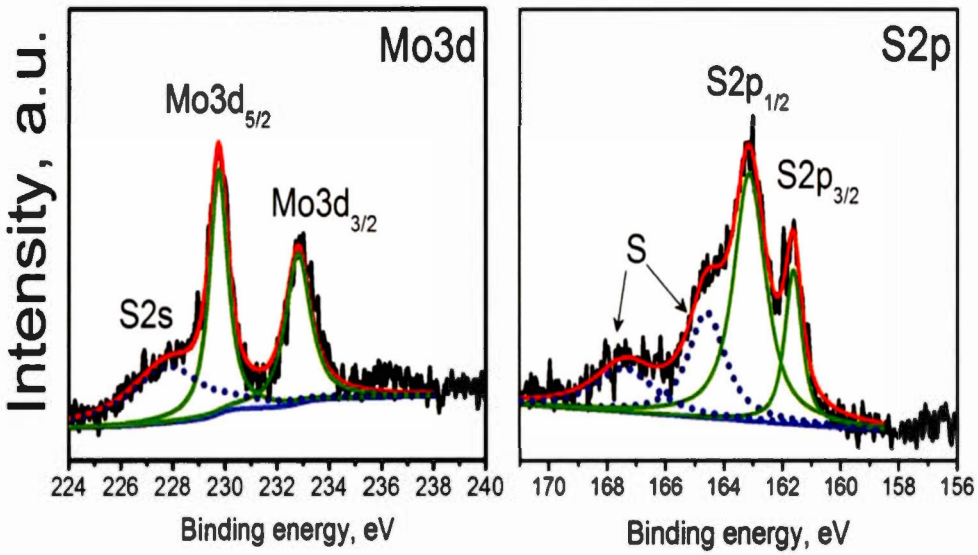

Figure 4.16 Shows the fitted high resolution S 2p and Mo 3d XPS peaks

CHAPTER V

ELECTRICAL PROPERTIES OF MOS_2

5.1 The field-effect transistor (FET) definition and operation

Field effect transistors (FETs) are the type of transistor based semiconductor materials in which the transistor use an electric field to control the electrical behavior of the device. It is made through p and n type semiconductors. FET is a unipolar transistor by which an electrical field is used to control the conductivity between its terminals; the source and the drain, by creating a voltage difference. Even though many types of this kind of transistors have been developed, there are two major classes; the metal oxide semiconductor (MOSFET) and the junction (JFET). FET has a high gate to the main current resistance results in a high degree of isolation between control and flow. However, its a relatively low gain bandwidth product as well as its low susceptibility to overload voltages, so it needs handling during installation (Colinge et al., 2010).

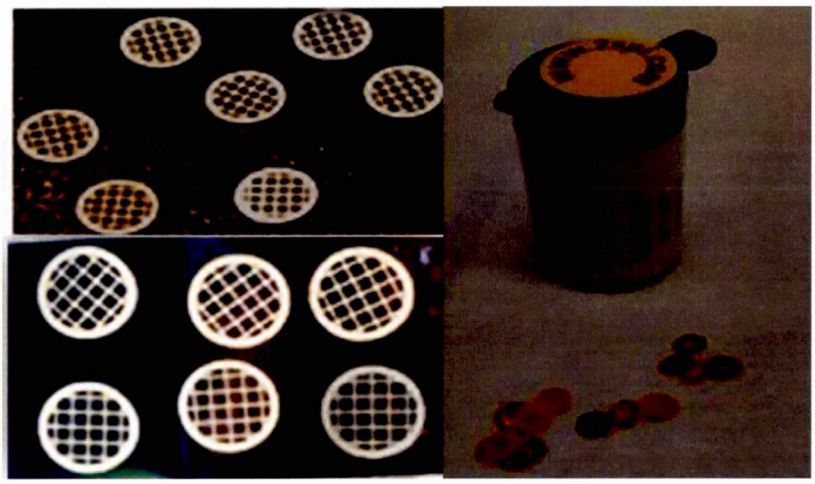

Figure 5.17 Images show TEM grides masks used to deposed elctodes on top of MoS_2 samples

5.2 FET Fabrication Method

In this study, the MoS_2 FETs were supported on Si/SiO_2 substrates using the SiO_2 (300 nm thermal oxide) as the dielectric layer and p+ doped Si ($\rho < 3 \times 10^{-3}$ □Ω cm) as the gate electrode. After the CVD growth of MoS_2, we proceed to TEM grids aligninement. To align TEM grid into the desired location, the TEM grid was stuck to a hole (1 mm diameter) punched in a Scotch Tape (1 mm thick) as shown in Figure 5.2, as the Scotch Tape is sticky to SiO_2 surfaces. Cr (5 nm) and Au (50 nm) contact pads of the FET devices were evaporated on top of MoS_2 layer through square holes of the TEM grid used as a shadow mask (see Figure 5.1).

After electrodes (source and drain) evaporation, we remove the scotch tape and the TEM grids (see Figure 5.3). After that, we placed the devices on a probe station (see Figure 5.4). The electrical probe station allows for quick and easy testing of individual FET on a variety of electrode designs. The unit is composed of two main sections, the XYZ position stages and the low-noise probe board. The substrate is loaded into the substrate holder, mounted on top of the vertical stage, and is kept firmly in position by two probes acting as source and drain contacts. The bottom and the edge of the holder provide an alternative route to electrically connect the gate to the Source Measurement Units.

Figure 5.18 The image of MoS_2 FET devices after depositing a gold electrode on the sample

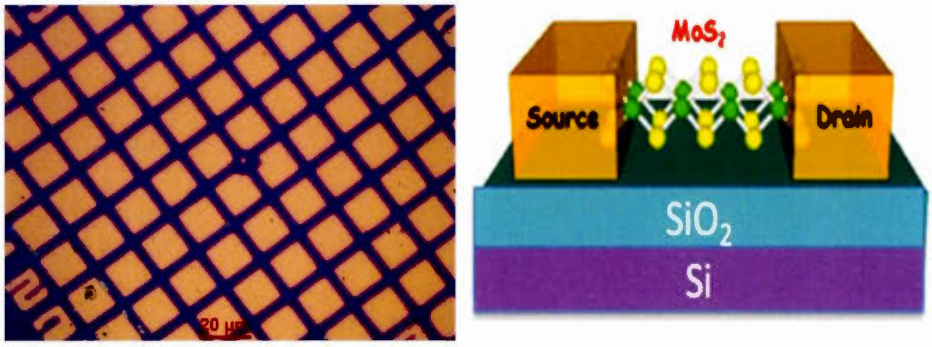

Figure 5.19 Shown device fabrication of MoS_2 (Das, Chen, Penumatcha, & Appenzeller, 2012)

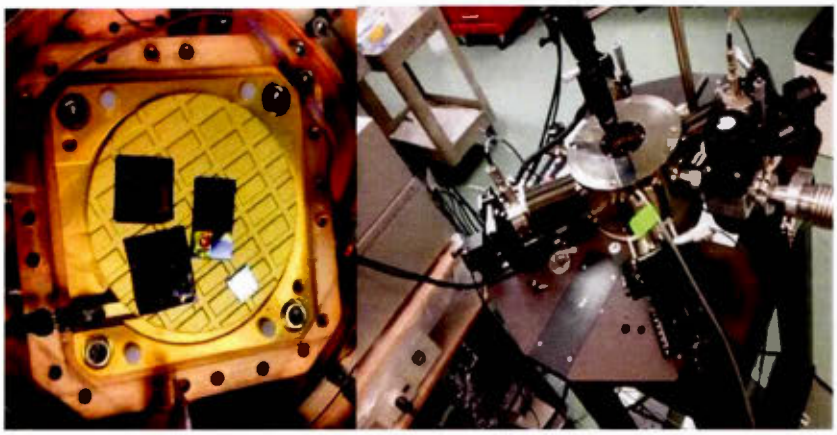

Figure 5.20 Probe station system

5.3 FET measurement of MoS_2 films.

A bias voltage was applied between the source and drain terminals of the MoS_2 channel. The Si substrate was used as a global back-gate; this bias field controls the carrier concentration and polarity in the MoS_2 monolayer. The voltage applied to gate terminal was swept continuously during the measurements. The output signal was used

to plot the graph. We found that the produced transistor behavior of MoS_2 showing a great output characteristics MoS_2 FETs under different gates voltage from 10 V to 40 V as shown in Figure 5.21. shows the output characteristics of a MoS_2 device, when Ids as a function of Vds at selected back-gate voltages between 10 and 40 V. The Id vs Vd measurements exhibit strongly non-linear (upward turning) Ids–Vds behavior, suggesting the presence of a significant schottky barrier at the contacts (see Figure 5.5).

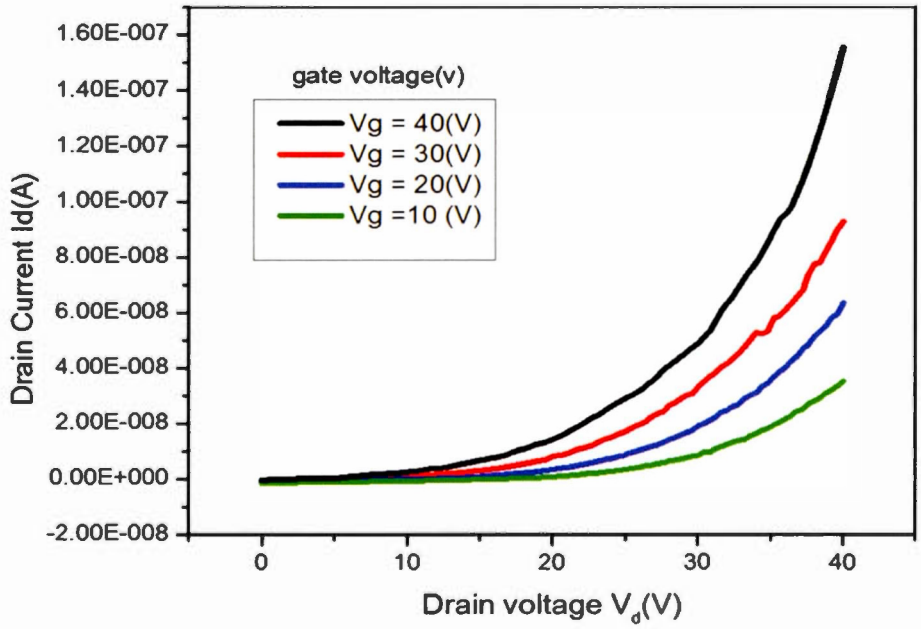

Figure 5.5 Output characteristics Id vs. drain voltage Vd with different gate voltage from 10 to 40V

In this study we found the field effect mobility of a single layer and monolayer MoS_2 device can be calculated from the following equation:

$$\mu = \frac{L\ (gm)}{W\ (CE\ VDS)}$$

Where L is the channel length (50 μm) and W is the channel width (300 μm) and for C_E is the capacitance between the channel and the gate (11.5 nf /cm^2) and for the V_{DS} voltage of drain around 1 eV. Moreover, g_m, the transconductance, equals to $g_m = \frac{dI_{DS}}{dV_{GS}}$ between source and drain voltage V_{dS} ,(Kappera et al., 2014)

The monolayer MoS_2 FET measurement with the thickness of oxide (SiO_2) around 300 nm on the sample with two gold electrodes acts as drain and the other source. We found that our devices exhibit high mobility from 0.11 to 8.4 $cm^2\ S^{-1}$. We should mention that we succeed in getting these values without using hafnium oxide HfO_2 at room temperature, compared with previous works on the MoS_2 mobility of single layer MoS_2 with the band gap 1.8 eV (Mak, Lee, Hone, Shan, & Heinz, 2010) they found the mobility range from 0.5-3 $cm^2\ S^{-1}$, (K. Novoselov et al., 2005), recently in last research reports using the hafnium oxide to improve the mobility of single-layer MoS_2 mobility of at least 200 $cm^2\ V^{-1}\ s^{-1}$, and this is similar to graphene, and also they found the mobility of 0.11 $cm^2\ v^{-1}\ s^{-1}$ from (Radisavljevic et al., 2011)

CONCLUSION

We have successfully synthesized MoS_2 flakes using Chemical Vapour Deposition process. We used different growth temperatures and different conditions to grow MoS_2 domains. The quality of the synthesized MoS_2 was systematically investigated with various characterization techniques to find a successful way to grow MoS_2 flakes with a large area of counting film. We used two furnaces for our CVD process, we used the first furnace for sulfur introduction (sublimation) at low temperatures (120 C° to 300 C°) and the second furnace for MoO_3 powder evaporation at high temperatures (between 650 C° to 800 C°) for 10 minutes. Based in all characterization techniques used for this work, we found that the quality of the growth MoS_2 exceeds the one reported in several publications. The FETs fabricated from our MoS_2 monolayer show great behavior as transistors with high mobility around 8.4 cm^2 S^{-1}. Indeed, MoS_2 as nano material has a sizable band gap, which is suitable as active layers in logic electronics and optoelectronics, it can be used as a constituent in a variety of energy-related applications for two-dimensional materials.

As we can see from the data, to grow large areas of MoS_2 the best condition found to be 750 C° like growth temperature for 10 minutes.This condition gives high quality and a large area of MoS_2 thin film. In conclusion, the CVD method is the best method to grow a MoS_2 monolayer and 2D materials in general.

REFERENCES

Anbazhagan, R., Wang, H.-J., Tsai, H.-C., & Jeng, R.-J. (2014). Highly concentrated mos 2 nanosheets in water achieved by thioglycolic acid as stabilizer and used as biomarkers. *RSC Advances, 4*(81), 42936-42941.

Ataca, C., Sahin, H., & Ciraci, S. (2012). Stable, single-layer mx2 transition-metal oxides and dichalcogenides in a honeycomb-like structure. *The Journal of Physical Chemistry C, 116*(16), 8983-8999.

Baugher, B. W., Churchill, H. O., Yang, Y., & Jarillo-Herrero, P. (2013). Intrinsic electronic transport properties of high-quality monolayer and bilayer mos2. *Nano letters, 13*(9), 4212-4216.

Binnig, G., Quate, C. F., & Gerber, C. (1986). Atomic force microscope. *Physical review letters, 56*(9), 930.

Brito, J. L., Ilija, M., & Hernández, P. (1995). Thermal and reductive decomposition of ammonium thiomolybdates. *Thermochimica acta, 256*(2), 325-338.

Chhowalla, M., Shin, H. S., Eda, G., Li, L.-J., Loh, K. P., & Zhang, H. (2013). The chemistry of two-dimensional layered transition metal dichalcogenide nanosheets. *Nature chemistry, 5*(4), 263-275.

Choy, K. (2003). Chemical vapour deposition of coatings. *Progress in materials science, 48*(2), 57-170.

Coleman, J. N., Lotya, M., O'Neill, A., Bergin, S. D., King, P. J., Khan, U., . . . Smith, R. J. (2011). Two-dimensional nanosheets produced by liquid exfoliation of layered materials. *Science, 331*(6017), 568-571.

Das, S., Chen, H.-Y., Penumatcha, A. V., & Appenzeller, J. (2012). High performance multilayer mos2 transistors with scandium contacts. *Nano letters, 13*(1), 100-105.

Dungey, K. E., Curtis, M. D., & Penner-Hahn, J. E. (1998). Structural characterization and thermal stability of mos2 intercalation compounds. *Chemistry of Materials, 10*(8), 2152-2161.

Eda, G., Yamaguchi, H., Voiry, D., Fujita, T., Chen, M., & Chhowalla, M. (2011). Photoluminescence from chemically exfoliated mos2. *Nano letters, 11*(12), 5111-5116.

Edwards, H. G., & Chalmers, J. M. (2005). *Raman spectroscopy in archaeology and art history* (Vol. 9): Royal Society of Chemistry.

Feng, Y., Zhang, K., Wang, F., Liu, Z., Fang, M., Cao, R., . . . Han, Y. (2015). Synthesis of large-area highly crystalline monolayer molybdenum disulfide with tunable grain size in a h2 atmosphere. *ACS applied materials & interfaces, 7*(40), 22587-22593.

Gourmelon, E., Lignier, O., Hadouda, H., Couturier, G., Bernede, J., Tedd, J., . . . Salardenne, J. (1997). Ms 2 (m= w, mo) photosensitive thin films for solar cells. *Solar energy materials and solar cells, 46*(2), 115-121.

Ho, W., Yu, J. C., Lin, J., Yu, J., & Li, P. (2004). Preparation and photocatalytic behavior of mos2 and ws2 nanocluster sensitized tio2. *Langmuir, 20*(14), 5865-5869.

Huang, X., Zeng, Z., & Zhang, H. (2013). Metal dichalcogenide nanosheets: Preparation, properties and applications. *Chemical Society Reviews, 42*(5), 1934-1946.

Jacobs-Gedrim, R. (2015). *Two-dimensional chalcogenides: Material synthesis and nano-device applications*: State University of New York at Albany.

Joensen, P., Frindt, R., & Morrison, S. R. (1986). Single-layer mos2. *Materials research bulletin, 21*(4), 457-461.

Kappera, R., Voiry, D., Yalcin, S. E., Branch, B., Gupta, G., Mohite, A. D., & Chhowalla, M. (2014). Phase-engineered low-resistance contacts for ultrathin mos2 transistors. *Nature materials, 13*(12), 1128-1134.

Kibsgaard, J., Chen, Z., Reinecke, B. N., & Jaramillo, T. F. (2012). Engineering the surface structure of mos2 to preferentially expose active edge sites for electrocatalysis. *Nature materials, 11*(11), 963.

Kuc, A., Zibouche, N., & Heine, T. (2011). Influence of quantum confinement on the electronic structure of the transition metal sulfide t s 2. *Physical Review B, 83*(24), 245213.

Lee, Y. H., Zhang, X. Q., Zhang, W., Chang, M. T., Lin, C. T., Chang, K. D., . . . Li, L. J. (2012). Synthesis of large-area mos2 atomic layers with chemical vapor deposition. *Advanced Materials, 24*(17), 2320-2325.

Li, Y., Wang, H., Xie, L., Liang, Y., Hong, G., & Dai, H. (2011). Mos2 nanoparticles grown on graphene: An advanced catalyst for the hydrogen evolution reaction. *Journal of the American Chemical Society, 133*(19), 7296-7299.

Lin, Y.-M., Dimitrakopoulos, C., Jenkins, K. A., Farmer, D. B., Chiu, H.-Y., Grill, A., & Avouris, P. (2010). 100-ghz transistors from wafer-scale epitaxial graphene. *Science, 327*(5966), 662-662.

Liu, H., Wong, S. L., & Chi, D. (2015). Cvd growth of mos2-based two-dimensional materials. *Chemical Vapor Deposition, 21*(10-11-12), 241-259.

Liu, K.-K., Zhang, W., Lee, Y.-H., Lin, Y.-C., Chang, M.-T., Su, C.-Y., . . . Zhang, H. (2012). Growth of large-area and highly crystalline mos2 thin layers on insulating substrates. *Nano Lett, 12*(3), 1538-1544.

Lopez-Sanchez, O., Lembke, D., Kayci, M., Radenovic, A., & Kis, A. (2013). Ultrasensitive photodetectors based on monolayer mos2. *Nature nanotechnology, 8*(7), 497-501.

Lv, R., Robinson, J. A., Schaak, R. E., Sun, D., Sun, Y., Mallouk, T. E., & Terrones, M. (2014). Transition metal dichalcogenides and beyond: Synthesis, properties, and applications of single-and few-layer nanosheets. *Accounts of chemical research, 48*(1), 56-64.

Ma, Y., Kou, L., Li, X., Dai, Y., & Heine, T. (2016). Two-dimensional transition metal dichalcogenides with a hexagonal lattice: Room-temperature quantum spin hall insulators. *Physical Review B, 93*(3), 035442.

Mak, K. F., Lee, C., Hone, J., Shan, J., & Heinz, T. F. (2010). Atomically thin mos 2: A new direct-gap semiconductor. *Physical review letters, 105*(13), 136805.

NANO, A. (12 july 2013). Molybdenum disulfide (mos2) nanoparticles - properties, applications. Retrieved from https://www.azonano.com/article.aspx?ArticleID=3351

Novoselov, K., Jiang, D., Schedin, F., Booth, T., Khotkevich, V., Morozov, S., & Geim, A. (2005). Two-dimensional atomic crystals. *Proceedings of the National Academy of Sciences of the United States of America, 102*(30), 10451-10453.

Novoselov, K. S., Geim, A. K., Morozov, S. V., Jiang, D., Zhang, Y., Dubonos, S. V., . . . Firsov, A. A. (2004). Electric field effect in atomically thin carbon films. *science, 306*(5696), 666-669.

Radisavljevic, B., Radenovic, A., Brivio, J., Giacometti, i. V., & Kis, A. (2011). Single-layer mos2 transistors. *Nature nanotechnology, 6*(3), 147-150.

Ramakrishna Matte, H., Gomathi, A., Manna, A. K., Late, D. J., Datta, R., Pati, S. K., & Rao, C. (2010). Mos2 and ws2 analogues of graphene. *Angewandte Chemie International Edition, 49*(24), 4059-4062.

Sheu, A.-D. (2015). Growth of mos2 layers by two-step chemical vapor deposition.

Shi, Y., Li, H., & Li, L.-J. (2015). Recent advances in controlled synthesis of two-dimensional transition metal dichalcogenides via vapour deposition techniques. *Chemical Society Reviews, 44*(9), 2744-2756.

Smith, E., & Dent, G. (2013). *Modern raman spectroscopy: A practical approach*: John Wiley & Sons.

Song, L., Ci, L., Lu, H., Sorokin, P. B., Jin, C., Ni, J., . . . Yakobson, B. I. (2010). Large scale growth and characterization of atomic hexagonal boron nitride layers. *Nano letters, 10*(8), 3209-3215.

Stankovich, S., Dikin, D. A., Piner, R. D., Kohlhaas, K. A., Kleinhammes, A., Jia, Y., . . . Ruoff, R. S. (2007). Synthesis of graphene-based nanosheets via chemical reduction of exfoliated graphite oxide. *carbon, 45*(7), 1558-1565.

Steinhoff, A., Kim, J.-H., Jahnke, F., Rosner, M., Kim, D.-S., Lee, C., . . . Gies, C. (2015). Efficient excitonic photoluminescence in direct and indirect band gap monolayer mos2. *Nano letters, 15*(10), 6841-6847.

Taheri, P. (2015). *Growth and optoelectronic properties of large-scale monolayer mos 2.* State University of New York at Buffalo,

Tedstone, A. A., Lewis, D. J., Hao, R., Mao, S.-M., Bellon, P., Averback, R. S., . . . Gaemers, S. (2015). Mechanical properties of molybdenum disulfide and the effect of doping: An in situ tem study. *ACS applied materials & interfaces, 7*(37), 20829-20834.

Wang, Q. H., Kalantar-Zadeh, K., Kis, A., Coleman, J. N., & Strano, M. S. (2012). Electronics and optoelectronics of two-dimensional transition metal dichalcogenides. *Nature nanotechnology, 7*(11), 699-712.

Xu, H.-J., Mi, J.-S., Li, Y., Zhang, B., Cong, R.-D., Fu, G.-S., & Yu, W. (2017). Nucleation mechanism and morphology evolution of mos2 flakes grown by chemical vapor deposition. *Chinese Physics B, 26*(12), 128102.

Xu, W.-b., Huang, B.-j., Li, P., Li, F., Zhang, C.-w., & Wang, P.-j. (2014). The electronic structure and optical properties of mn and b, c, n co-doped mos 2 monolayers. *Nanoscale research letters, 9*(1), 554.

Yang, X., Li, J., Liang, T., Ma, C., Zhang, Y., Chen, H., . . . Xu, M. (2014). Antibacterial activity of two-dimensional mos 2 sheets. *Nanoscale, 6*(17), 10126-10133.

Yin, Z., Li, H., Li, H., Jiang, L., Shi, Y., Sun, Y., . . . Zhang, H. (2011). Single-layer mos2 phototransistors. *ACS nano, 6*(1), 74-80.

Zeng, Z., Yin, Z., Huang, X., Li, H., He, Q., Lu, G., . . . Zhang, H. (2011). Single-layer semiconducting nanosheets: High-yield preparation and device fabrication. *Angew Chem Int Ed Engl, 50*(47), 11093-11097. doi:10.1002/anie.201106004

Zeng, Z., Yin, Z., Huang, X., Li, H., He, Q., Lu, G., . . . Zhang, H. (2011). Single-layer semiconducting nanosheets: High-yield preparation and device fabrication. *Angewandte Chemie International Edition, 50*(47), 11093-11097.

Zhan, Y., Liu, Z., Najmaei, S., Ajayan, P. M., & Lou, J. (2012). Large-area vapor-phase growth and characterization of mos2 atomic layers on a sio2 substrate. *Small, 8*(7), 966-971.

Zheng, J., Liu, H.-T., Wu, B., Di, C.-A., Guo, Y.-L., Wu, T., . . . Zhu, D.-B. (2012). Production of graphite chloride and bromide using microwave sparks. *Scientific reports, 2*, 662.

Zhou, L., Cai, M., Tong, T., & Wang, H. (2017). Progress in the correlative atomic force microscopy and optical microscopy. *Sensors, 17*(4), 938.